Journal of Marine Systems 134 (2014) 29–44

Contents lists available at ScienceDirect

Journal of Marine Systems

journal homepage: www.elsevier.com/locate/jmarsys

Nutrient input and the competition between *Phaeocystis pouchetii* and diatoms in Massachusetts Bay spring bloom

Mingshun Jiang [a,*], David G. Borkman [b], P. Scott Libby [c], David W. Townsend [d], Meng Zhou [a]

[a] School for the Environment, University of Massachusetts Boston, 100 Morrissey Blvd., Boston, MA 02125, USA
[b] Graduate School of Oceanography, University of Rhode Islands, 215 South Ferry Road, Narragansett, RI 02882, USA
[c] Battelle Memorial Institute, 397 Washington St., Duxbury, MA 02332, USA
[d] School of Marine Sciences, 5706 Aubert Hall, University of Maine, Orono, ME 04469, USA

ARTICLE INFO

Article history:
Received 12 October 2013
Received in revised form 19 February 2014
Accepted 20 February 2014
Available online 1 March 2014

Keywords:
Nutrients
Diatoms
P. pouchetii
Massachusetts Bay
Gulf of Maine
Spring bloom
Winter storm
River discharges
North Atlantic Oscillations
Ecosystem model

ABSTRACT

The phytoplankton community in Massachusetts Bay has displayed significant inter-annual variability and possible trends over the last two decades, with increasing frequency and magnitude of strong *Phaeocystis pouchetii* blooms and generally opposite fluctuations in diatom abundances. An analysis of historical data suggests that changes in winter nitrate and silicate concentrations (both their absolute and relative values) may play a critical role in the competition between diatoms and *P. pouchetii*. We developed a new ecosystem model to simulate *Phaeocystis* dynamics and to test the significance of variable winter nutrient levels. Idealized simulations for the years 1992–2009 generally reproduced the observed inter-annual variability of *P. pouchetii* and diatoms during the spring blooms, with modeled peaks in biomass of diatoms and *P. pouchetii* significantly being correlated with their observed mean abundances. Moreover, modeled peak biomass ratio and observed mean abundance ratio between diatoms and *P. pouchetii* during the spring blooms were similarly depending on both the winter nitrate and residual nitrate (nitrate minus silicate) concentrations. These results are consistent with resource competition theory in which relatively low winter nutrient concentrations would favor species with faster growth rate (diatoms, in this case). With sufficiently high winter nutrient concentrations, however, *P. pouchetii* was able to grow before nitrate being depleted by diatoms, even though winter Si > N. Our observations further indicate that inter-annual nutrient variability and consequently spring bloom phytoplankton variability in Massachusetts Bay are likely driven by changes in winter nutrient fluxes from Gulf of Maine rivers and winter convective mixing. These fluxes may have been modulated by large-scale processes such as the North Atlantic Oscillations and Arctic melting through the river discharges, winter-storm activities (and hence winter mixing and nutrient supply), and the deep waters inflow into the Gulf of Maine.

1. Introduction

Massachusetts Bay (MB) is a coastal embayment in the western Gulf of Maine (GOM) (Fig. 1). Recent studies indicated that the phytoplankton community in the bay displayed strong inter-annual variability and possible trends over the last two decades (Hunt et al., 2010). In particular, both the frequency and magnitude of *Phaeocystis pouchetii* blooms have increased with diatom and *P. pouchetii* abundances largely fluctuating in opposite phase. Yet, the dynamic mechanisms leading to such changes remain unclear. Given the different nutrient requirements of diatoms and *P. pouchetii*, one potential mechanism is the nutrient competition between these two species (e.g. Egge and Aksnes, 1992; Lancelot and Rousseau, 1994; Officer and Ryther, 1980; Wilson et al., 2007).

Circulation in MB is driven by local forcing (winds and runoff) and the GOM intruding current around Cape Ann (Fig. 1), which is a branch of the western Maine Coastal Current (WMCC), a buoyancy- and wind–driven current that extends from the eastern Maine Coastal Current (EMCC) (Bigelow, 1927; Brooks, 1985; Geyer et al., 1992, 2004; Lynch et al., 1997; Pettigrew et al., 2005). The WMCC also includes contributions from a coastal freshwater plume driven by river discharges. In spring, strong river runoff and downwelling favorable winds produce a narrower and stronger coastal jet and an enhanced intruding flow (Churchill et al., 2005; Geyer et al., 2004). The jet may separate from the coastline to form meso-scale eddies in the North Passage (Jiang et al., 2011). During winter and spring, the intruding current from the GOM tends to extend southward along the MB coast, and sometimes can penetrate deeply into Cape Cod Bay. Thus, MB is a semi-enclosed system with strong input from the GOM through the North Passage.

* Corresponding author at: Harbor Branch Oceanographic Institute, Florida Atlantic University, 5600 US 1 North, Ft. Pierce, FL 34946, USA. Tel.: +1 772 242 2254; fax: +1 772 242 2412.
E-mail address: jiangm@fau.edu (M. Jiang).

http://dx.doi.org/10.1016/j.jmarsys.2014.02.011
0924-7963/

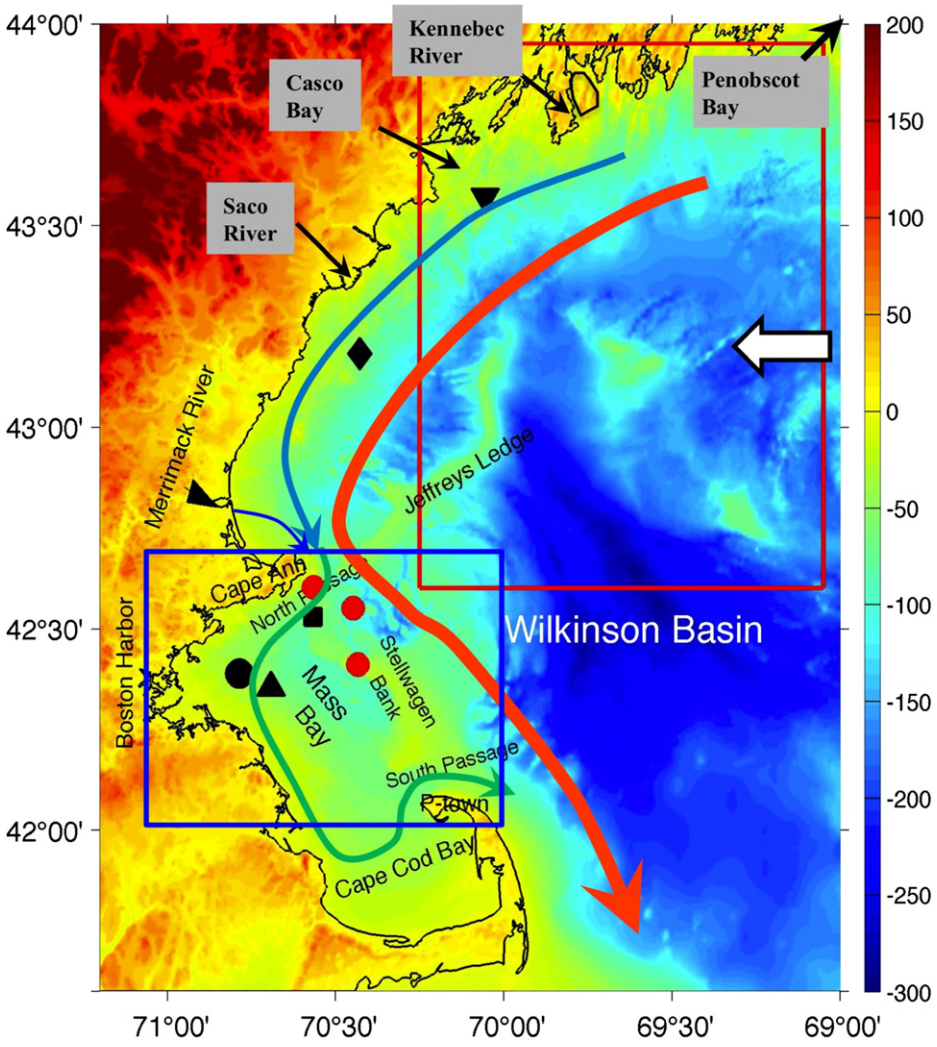

Fig. 1. Bathymetry (color) and circulation (broad arrows) in the western GOM and MB. Symbols: MWRA outfall (black dot), GoMOOS-buoy A, B, and C (square, diamond, and downward triangle), NDBC buoy 44013 (black triangle), and MWRA stations F26–28 (red dots) along the MB boundary (other stations not shown). Red box indicates the conceptual MB nutrient source area, and blue box indicates our western MB study area. Broad arrows highlight the general circulation pattern including GOM coastal plume (blue, high Si/N), WMCC (red, low Si/N), Merrimack River plume (deep blue, high Si/N), and MB coastal current including the GOM intruding current (green, median Si/N). Broad open arrow indicates input from the eastern Gulf of Maine including EMCC and transport of GOM deep waters.

The MB ecosystem is strongly influenced by the water, nutrients and zooplankton inputs from the GOM intruding current (Jiang et al., 2007a, b). In particular, nutrient input from the GOM constitutes the primary source for MB nutrients, with additional contribution from river discharges in Boston Harbor and the Boston sewage effluent (HydroQual and Normandeau, 1995). Therefore, we may expect a significant influence of the GOM nutrient input on the abundance and species composition in the MB phytoplankton community. Furthermore, the coastal current may propagate signals of large-scale processes into MB through transport of water, nutrients, and biota.

Phytoplankton in MB exhibit a strong seasonal cycle with typically strong spring and fall blooms. The spring bloom normally occurs in late March and early April while the fall bloom occurs in October and early November, both are dominated by diatoms species and both show strong inter-annual variations in magnitude (Hunt et al., 2010; Jiang et al., 2007a; Keller et al., 2001; Townsend et al., 1994). Surface nutrients, especially dissolved inorganic nitrogen (DIN), are nearly depleted following spring bloom and late spring and summer primary production is relatively low, with a phytoplankton assemblage dominated by small flagellates (e.g. Libby et al., 2007). *P. pouchetii* populations had been recorded during the spring bloom in 1990s, but the abundances had been relatively low. In recent years, however, *P. pouchetii* has become a more important component of the MB phytoplankton community during the spring bloom, with mean abundances in some years exceeding 2×10^6 cells L^{-1} (e.g., Hunt et al., 2010; Libby et al., 2007, 2008). These *P. pouchetii* blooms are more confined to western portion of MB, waters fed by the GOM intruding current.

Both diatoms and *Phaeocystis* are important to the global carbon cycle and production of dimethylsuflide (DMS; e.g. Arrigo et al., 1999; Smith et al., 1991; Stefels, 1997; Townsend and Keller, 1996). *Phaeocystis* blooms were typically viewed as a nuisance phenomenon, sometimes forming foam on beaches. Recent studies have suggested that *Phaeocystis* colonies have high hemolytic lipid content, which may be toxic to fish larvae (Eilertsen and Raa, 1995; Hansen et al., 2003; Stabell et al., 1999; van Rijssel et al., 2007). Intense *Phaeocystis* blooms may also affect benthic communities by depleting bottom dissolved oxygen following the demise of the blooms and the sinking of cells to the bottom (Rogers and Lockwood, 1990; Spilmont et al.,

2009). It is therefore important to gain a better understanding of the probable causes underlying the recent changes to more frequent and intense *P. pouchetii* blooms in MB.

We present here an analysis of the long-term (1992–2009) nutrient and phytoplankton data in MB collected by the Massachusetts Water Resource Authority (MWRA) and others, as well as auxiliary hydrological and meteorological data. A new ecosystem model was developed and a series of idealized zero-dimensional (0-D), i.e. horizontally uniform, two-layer numerical simulations for the 18 years was carried out. The observed and modeled results are interpreted in the context of resource competition theory (e.g. Tilman, 1977, 1982). The goal is to understand the relationships among nutrients, phytoplankton abundance and species composition during the MB spring bloom and to understand the underlying dynamic mechanisms for the observed phytoplankton changes. The focus in this study was winter nutrients, although we were aware that other factors such as light, temperature, mixing, and zooplankton may also affect the bloom development.

In order to understand the potential external driving force for the phytoplankton changes, we also examined the external processes including the GOM river discharges, and winter convective mixing, and studied their impacts on the nutrient fields in the western GOM and consequently the MB spring phytoplankton bloom. A discussion of potential influences of large-scale processes such as the North Atlantic Oscillations (NAO) and Arctic melting on the regional nutrient fluxes and the MB phytoplankton bloom is also presented.

2. Methods

2.1. Data

Long-term nutrient and phytoplankton data used here were collected by the MWRA as a part of the monitoring program in MB, which includes 17 survey cruises per year (reduced to 12 per year since 2004) sampling at 21 stations (reduced to 7 since 2004) near the MWRA outfall (Fig. 1). Among these cruises, 6 of them visited an additional 27 stations encompassing the entire bay, with two cruises scheduled during the winter–spring period (see, e.g. Libby et al., 1999). In addition to standard hydrographic measurements, water samples were collected at five standard depths (<3 m, half-way between surface and mid-depth, mid-depth, halfway between mid-depth and bottom, and near bottom (within 5 m of bottom)) for determining concentrations of phytoplankton chlorophyll, nutrients, organic matter, and dissolved oxygen. Unfiltered water samples (1 L) were collected and preserved in 1% Lugol's solution (Utermöhl, 1958) for phytoplankton identification and enumeration, and 102 μm mesh net tows for zooplankton abundance and identification were conducted at a subset of stations. Phytoplankton cell numbers were counted to species level when possible. Both *P. pouchetii* unicell and colonial forms were detected, but the populations (in term of biomass) were overwhelmingly dominated (estimated >95%) by the colonial forms. Within each colony observed, individual *P. pouchetii* cells were enumerated through focusing on the colonies at 500× magnification. Detailed descriptions of field sampling and laboratory analyses are given in Hunt et al. (2010).

The winter mean nutrient concentrations in western MB, defined as a box (71–70°W, 42.0–42.8°N) (Fig. 1), were computed based on observations during February–March for the upper 40 m, a depth chosen to approximate the surface mixed layer depth (MLD) this time of the year. These values are treated as pre-bloom nutrient concentrations. Total diatom and *P. pouchetii* cells in western MB were also calculated from field data collected during March–April period, which is typically the time of the spring bloom. Then the average abundances with the box were computed for all the samples analyzed over the two-month period. In some cases, zero or very low cell counts of *P. pouchetii* were observed. Therefore, an arbitrarily low number (1×10^4 cells) was used in order to avoid the singularity during logarithmic transformation for the data analysis.

We have also included nutrient measurements at the three MWRA stations along the northern boundary of MB (Fig. 1) in our analysis on the impacts of the nutrient input from the GOM. At these stations, there was only one MWRA survey, during mid-February, before the spring bloom each year. The correlations were computed between those nutrient data, the Merrimack River winter flow data recorded at the United States Geological Survey (USGS) gauge at Lowell, Massachusetts, and the surface wind data at the National Oceanic and Atmospheric Administration (NOAA) National Data Buoy Center (NDBC) buoy 44013 (Fig. 1) over the January to February period. Since there was no March nutrient data at these boundary stations, we did not include the March river or wind data.

Monthly climatological mean nutrient concentrations in the Merrimack River were computed based on the same USGS river database mentioned above over the period 1950–2009, which includes infrequent nutrient measurements about once per month. Although there are significant variations of nutrient concentrations among rivers along the GOM coast, they have similarly higher silicate than nitrate. For example, Hunt et al. (2005) reported a mean Si/N ratio of 5 for the Androscoggin and Kennebec Rivers, which is close to the mean 4.45 Si/N ratio measured at the USGS river gauge in the Merrimack River at Lowell, MA over the last 60 years. We used the nutrient values in the Merrimack River as a representative of nutrient concentrations for rivers around the western GOM. The nutrient concentrations for GOM deep waters were taken as those reported for spring of 1998 in Townsend et al. (2005).

The major nutrient sources to MB include primarily the GOM input, both at the surface and at depth, but also the MWRA effluent. A summary of these of these nutrient fluxes by source for the February–March period is given in Table 1. The MWRA input was computed as the time-averaged effluent rate (~20 m^3/s) multiplied by the average concentrations measured in 1993–1994 (Hunt et al., 1995). To estimate the GOM nutrient input, we used the mean GOM intruding flow during February–March 1995 from a three-dimensional numerical simulation (Jiang and Zhou, submitted for publication), and the mean nutrient concentrations of the MWRA February measurements during 1992–2009 at the two stations in the North Passage (Fig. 1). For river fluxes, we used the winter (December–February) mean combined flows of the three major rivers (Merrimack, Saco, Kennebec) in the western GOM (Fig. 1), and the mean nutrient concentrations in the Merrimack River measured at the USGS gauge at Lowell, MA.

2.2. Ecosystem model

Several *Phaeocystis* models have been developed ranging from simple NPZ type models (Arrigo et al., 2003; Walsh et al., 2001, 2004), moderately complex models that consider separately phytoplankton photosynthesis and growth (Lancelot et al., 2005), to complicated life cycle models (Whipple et al., 2007). We developed the first type of model based on the existing MB biogeochemical model, named Bay Eutrophication Model (BEM; HydroQual and Normandeau, 1995; Jiang et al., 2007b). The BEM was revised to simulate explicitly *P. pouchetii* and zooplankton (Fig. 2). The revised model included three types of phytoplankton including diatoms, *P. pouchetii*, and other autotrophic micro-flagellates, and two types of zooplankton (micro- and meso-zooplankton). *P. pouchetii* was modeled as both colonies (one group only) and solitary cells, but solitary cells were grouped into the micro-flagellate group (Fig. 2; Lancelot et al., 2005). In the model, colonies form as nutrients, light and temperature conditions become favorable, e.g. when light reaches a threshold level (Peperzak et al., 1998). Disrupted senescent colonies mostly become free flagellate cells with a portion of that biomass returning to the organic matter pool. Low grazing rates and relatively fast growth (compared to free cells) promote the initially rapid development of colonies. However, the *P. pouchetii* colonies are subject to faster sinking velocities and more

Table 1
Typical nutrient fluxes from MWRA effluent and GOM intruding flow during February–March.

	DIN		Silicate	
	Concentration (μM)	Flux (mol/s)	Concentration (μM)	Flux (mol/s)
MWRA[a]	1200	24	450	9
Intruding flow[b]	10[c]	400	10[c]	400
(river input)[d]	(40)	(32)	(178)	(142.4)
Atmospheric deposition[e]		14.5		0

[a] A MWRA mean effluent flow ~20 m^3/s is used, which is fairly stable over time (see, e.g., Jiang and Zhou, 2006a). The mean nutrient concentrations were derived from MWRA measurements during 1993–94 (Hunt et al., 1995). Overall, total DIN concentrations in the effluent have been little changes during 1995–2009, but there were no more measurements of silicate since then (Wu, 2011).
[b] The typical volume of GOM intruding flow in the Feb.–Mar. period is ~4×10^4 m^3/s (Jiang and Zhou, submitted for publication), which includes the river inputs in the western GOM.
[c] Typical nutrient concentrations were based on MWRA measurements at the two stations in the North Passage during 1992–2009 (see, e.g., Jiang and Zhou, 2006b).
[d] Part of the river inputs (within parenthesis) are included in the intruding flow, and the rest are transported downstream or into the Gulf. To estimate the contribution of river discharges, we used the long-term winter mean combined flow (~800 m^3/s) of the three major rivers (Merrimack, Saco, and Kennebec) in the western GOM. The mean river nutrient concentrations are derived from the USGS winter measurements in the Merrimack River from 1950 to present.
[e] Annual mean atmospheric N deposition is used, and silica deposition is assumed zero (see, e.g., Jiang and Zhou, 2006b).

severe viral lysis under nutrient stress and hence the modeled blooms generally didn't last long (Lancelot et al., 2005).

Two zooplankton components were added to the BEM to better represent grazing pressure on different phytoplankton groups: micro-zooplankton feeding upon microflagellates only, and meso-zooplankton feeding on micro-zooplankton, *P. pouchetii*, and diatoms. No species-specific zooplankton life cycle was considered. The formulation of meso-zooplankton grazing followed the preferential grazing formulation by Fasham et al. (1990) feeding primarily on micro-zooplankton and diatoms. Because of grazing resistance of *P. pouchetii* colonies, a small preference (<0.1) was used for meso-zooplankton feeding on *P. pouchetii* (Nejstgaard et al., 2007). A quadratic zooplankton mortality term was used to avoid unrealistic predator–prey interactions (Steele and Henderson, 1992).

Each model variable (e.g., N) in the water column follows the advection-diffusion-reaction equation,

$$dN/dt = \nabla\bullet\left(\vec{K}\bullet\nabla N\right) + \text{sources} - \text{sinks} \quad (1)$$

where d/dt represents the total derivative of the variable, $\vec{K}$ is a model diffusivity tensor, and the sources and sinks represent the biochemical reactions terms.

The detailed equations and model parameters can be found in Appendix A. Following are a few key equations. Phytoplankton photosynthesis follows the *P–I* curve proposed by Platt et al. (1980),

$$\mu_{\max} = P_{\max}\left(1 - e^{-\alpha I/P_{\max}}\right)e^{-\beta I/P_{\max}} \quad (2)$$

where I is the photosynthetically available radiation (PAR), α and β are the phytoplankton light assimilation efficiency and light inhibition coefficient, respectively, and $P_{\max}$ is the phytoplankton maximum growth rate. The maximum growth of phytoplankton is dependent on water temperature (Jiang et al., 2007b; Schoemann et al., 2005),

$$\mu'_{\max} = \mu_{\max}\exp\left(-(T - T_{OPT})^2/\Delta T^2\right) \quad (3)$$

where T_{OPT} and ΔT are the optimal temperature and associated interval for phytoplankton growth, respectively.

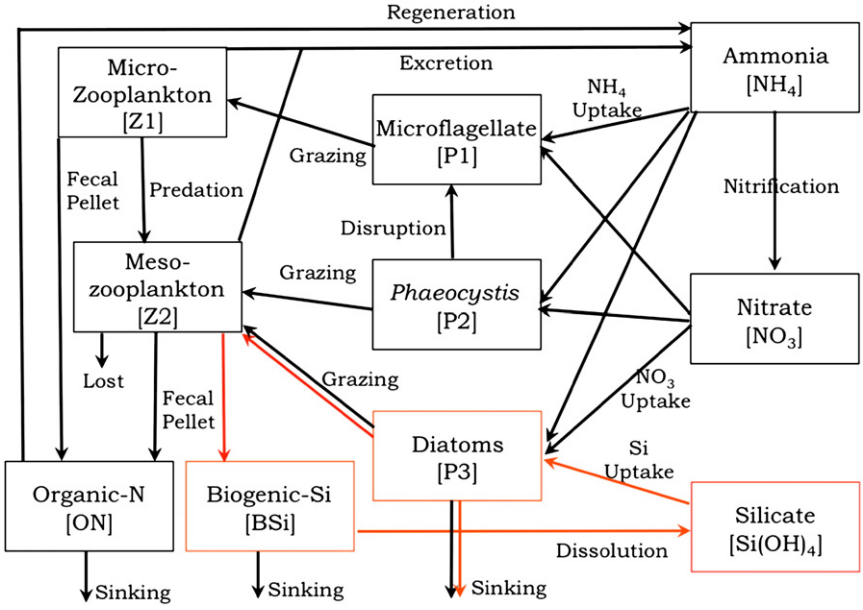

Fig. 2. A schematic of the biological model. Red lines indicate the silica flows. Note that some minor processes such as phytoplankton exudation and zooplankton respiration are not shown, and organic nitrogen components are grouped into one box for visualization convenience. We used a two-layer model for the water column and therefore the sediment component is not included.

Nutrient uptake was simulated with the Michaelis–Menten kinetics for both DIN and silicate,

$$\begin{cases} f_{DIN} = \dfrac{NO_3}{NO_3 + k_{NO3}} e^{-\varphi NH_4} + \dfrac{NH_4}{NH_4 + k_{NH4}} \\ f_{Si} = \dfrac{Si(OH)_4}{Si(OH)_4 + k_{Si(OH)_4}} \end{cases} \quad (4)$$

where ϕ is the ammonia inhibition coefficient (Fasham et al., 1990; Wheeler and Kokkinakis, 1990), and k_{NO_3}, k_{NH_4}, and $k_{Si(OH)_4}$ are the half saturation constants for uptake. Therefore, the nitrogen uptake for microflagellate and *P. pouchetii* follows,

$$\mu = \mu'_{max} f_{DIN}. \quad (5)$$

The actual uptake rate for diatoms is determined by Liebig's Law,

$$\mu = \mu'_{max} \min(f_{DIN}, f_{Si}). \quad (6)$$

The nutrient stress for *Phaeocystis* sedimentation and viral lysis was dependent on the available ambient nitrogen and the half saturation concentration (Lancelot et al., 2005),

$$N_{stress} = \max(k_{NO3}/(NO_3 + k_{NO3}), k_{NH4}/(NH_4 + k_{NH4})). \quad (7)$$

Choices of model parameter values were largely based on the existing BEM (Jiang et al., 2007b), available measured values for this region (Hegarty and Villareal, 1998; Townsend et al., 1992, 1994), or literature values (e.g., Lancelot et al., 2005; Sarthou et al., 2005; Schoemann et al., 2005). Both the micro- and meso-zooplankton grazing rates, and the meso-zooplankton mortality rates are based on measurements from the general area such as Georges Bank (Ohman et al., 2004, 2008) or from literature values for temperate species (Calbet, 2001; Calbet and Landry, 2004).

2.3. Numerical simulations

In this study, the water column was simplified as two layers: 1) surface mixed layer with the thickness defined by the MLD and 2) a bottom layer with an unlimited depth. Nutrients between the two layers were exchanged through vertical mixing, while particles including phytoplankton and detritus sank below the thermocline. Phytoplankton cells sinking out of the surface mixed layer were assumed to be dead immediately. Similar two-layer structures have been used in a number of previous modeling studies (e. g. Evans and Parslow, 1985; Fasham et al., 1990). The model was forced by specified physical parameters including MLD, short wave solar radiation, vertical mixing coefficient, and water temperature with their typical seasonal cycles in MB (see Appendix A).

Because this model is highly idealized (e.g. no horizontal advection) and is used only to demonstrate the phytoplankton responses to winter nutrients, we did not wish to conduct a long-term continuous simulation. Modeled results from such a simulation might drift too far away from what were set by the initial conditions. Therefore, we chose to simulate each year separately with different initial nutrient conditions. A series of numerical simulations were conducted for each of the 18 observational years (1992–2009), and both initial winter nitrate and silicate concentrations for each year were taken from the observed concentrations in that year. The initial values for all other biochemical variables were set to zero. Model results were taken from the second year of the simulations to allow for model adjustment. The winter nutrients in the second year were strongly correlated with the initial nutrients ($r^2 = 0.9$) (not shown). This model represents the over-all average conditions in the study area. Therefore the comparison with observations should also be interpreted as comparing the mean observed conditions, even though sampling stations vary in water depth and hydrodynamic, chemical, and biological conditions.

3. Results

3.1. Observed nutrients and phytoplankton in MB spring bloom

Since 1992, *P. pouchetii* abundances during the spring bloom in western MB have shown strong inter-annual variability, although there are significant spatial–temporal variations as reflected by the large standard deviations (Fig. 3a). *P. pouchetii* abundances have also shown a significant linear trend ($r = 0.49$, $p < 0.05$ for a linear regression with time). At the same time, diatom cell abundances during the spring bloom also showed a significant long-term decline over the last two decades ($r = -0.66$, $p < 0.01$ for a linear regression with time). The fluctuations of diatom abundances were inversely correlated with the *P. pouchetii* abundances ($r = -0.55$, $p < 0.05$).

Winter nitrate concentrations in MB also show significant inter-annual variability (Fig. 3b). Since 1992, the pre-bloom (Nov.–Feb.) nitrate concentrations in western MB have increased, while the silicate concentrations have fluctuated leading to overall increasing residual nitrogen (i.e. $[NO_3]$–$[Si(OH)_4]$) with a weak but significant linear trend (slope $s = 0.14$ μM/year, $r = 0.46$, $p < 0.05$) (Fig. 3c). *P. pouchetii* abundance during the spring bloom appears to have increased along with the pre-bloom nitrate concentrations and also with the N residual, while the

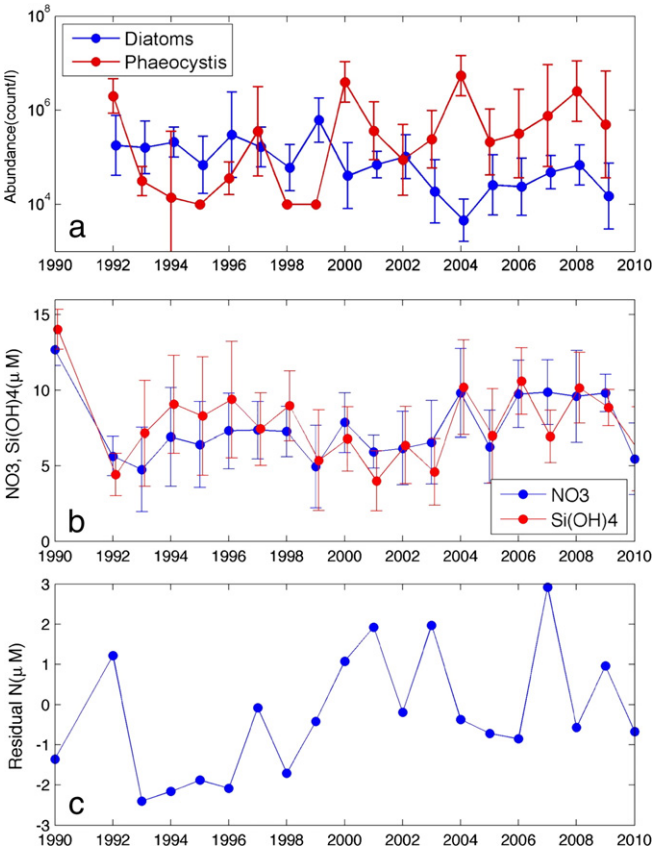

Fig. 3. a) Observed abundances of diatoms and *P. pouchetii* (an arbitrary 10^4 count/l is used for values $< 10^4$ count/l) in western MB during Mar.–Apr. period. Their standard deviations are also plotted. b) Pre-spring bloom (Nov.–Feb.) nitrate and silicate concentrations in western MB and their standard deviations. Note that for clarity, the error bars of diatoms and silicate are slightly shifted forward in time. c) The pre-bloom residual nitrogen (NO_3–$Si(OH)_4$) in western MB. No nutrient data in 1991.

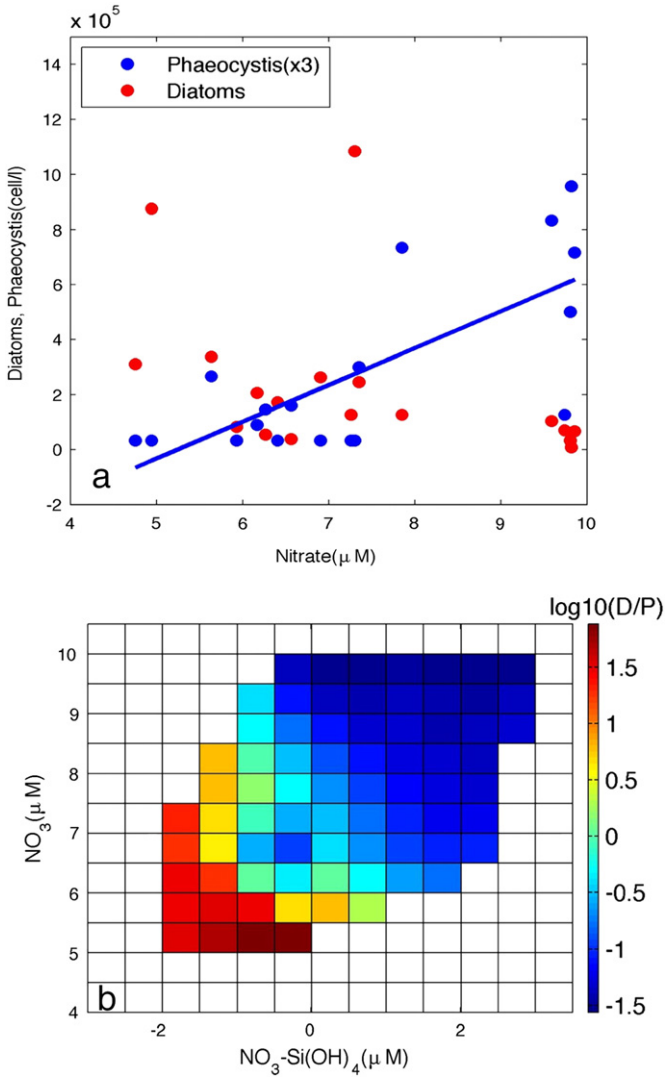

Fig. 4. (a) *P. pouchetii* and diatom abundances (Mar.-Apr.) versus nitrate (Nov-Feb.). *P. pouchetii* abundance is significantly correlated with nitrate ($r = 0.71$, $p < 0.05$), but not diatoms and (b) Relative abundances of diatom and *P. pouchetii* (log10(diatom/Phaeo)) versus N residual and nitrate. Both nitrate and N residual are important in controlling the *P. pouchetii* concentrations and the relative abundances between *P. pouchetii* and diatoms.

relative abundance of diatoms versus *P. pouchetii* decreases along with the increase of either absolute N concentrations or N residual ($r = 0.73$, $p < 0.01$ and $r = 0.54$, $p < 0.05$ respectively) (Fig. 4). In fact, a two-way ANOVA analysis found that the nitrate and residual nitrogen together could explain about 65% of the *P. pouchetii* variance observed.

3.2. Modeled phytoplankton responses to nutrients

To understand the responses of phytoplankton blooms to winter nutrient conditions, we used modeled results for year 2000 as an example year with moderately high winter nutrients and a moderate residual N ($NO_3 \sim 8$ μM and $Si(OH)_4 \sim 7$ μM, respectively) (Fig. 5). In this case, diatoms bloom in late March followed by a *P. pouchetii* bloom and silicate becomes depleted before nitrate. Both the diatom and *P. pouchetii* biomass are low in the summer but diatoms develop a strong fall bloom in October. Modeled flagellate biomass is low and nearly constant throughout the year. The meso-zooplankton biomass has a late spring and early summer peak while the micro-zooplankton biomass is low (not shown). These results generally agree with the observed patterns of nutrients and chlorophyll except for the short early summer diatom bloom triggered by nutrient inputs from spring freshets, a factor not included in the simulation (Fig. 5). No *P. pouchetii* blooms have been observed in MB along with the spring freshets. The reasons are unclear, but the warmer temperature (less favorable to *P. pouchetii* growth) at the time may have been a contributing factor.

Compared to 2000, winter nitrate and silicate concentrations in 2004 are relatively higher, about 10 μM and 8 μM, respectively, and there is also more residual N. In this case, modeled results show that a strong *P. pouchetii* bloom occurs nearly the same time as the diatom bloom with their peak biomass about the same because of higher pre-bloom nitrate than that in 2000 (Fig. 6a and b). The variability of both phytoplankton groups during the rest of 2004 is similar to 2000. It is noteworthy that in this case, nitrate is depleted while the minimum silicate concentration is about 2 μM. This is consistent with the observed nutrient and phytoplankton seasonal cycles during 2004 (Jiang and Zhou, 2006b). In contrast, when the pre-bloom nitrate concentration is relatively low as observed in 1995 ($NO_3 \sim 6$ μM and $Si(OH)_4 \sim 8$ μM, respectively), modeled results show that a *P. pouchetii* bloom fails to develop, while the diatoms have similar spring and fall blooms as in 2000 and 2004 case (Fig. 6c and d).

Modeled peak *P. pouchetii* biomass is generally consistent with the observed abundances, whereas modeled diatom biomass remains relatively constant over the years, in contrast to the observed decreasing trend in diatom abundances (Fig. 7). In relation to winter nitrate concentration, maximum *P. pouchetii* biomass is near zero at low winter nitrate levels but increases nearly linearly as winter nitrate concentrations are >6 μM, suggesting *P. pouchetii* becomes more competitive with diatoms at high nitrate concentrations (Fig. 8a). In contrast, the maximum diatom biomass appears to increase slightly with the winter nitrate concentration. Modeled peak *P. pouchetii* biomass is significantly correlated with their observed mean *P. pouchetii* abundances during March–April with $r = 0.71$ ($p < 0.01$). There is no correlation between modeled maximum diatom biomass and observed mean diatom abundances in March–April ($r = 0.3$, $p = 0.1$). In addition, no clear trend is detected for the modeled maximum diatom biomass in the last two decades, whereas observations in western MB seem to show a weak decline in peak diatom abundances during the spring bloom. The reason for such a discrepancy is unclear. The model may have over-estimated the diatoms loss terms (e.g. sinking and grazing) and hence underestimated diatom biomass under Si limitation situation. Overall, modeled relative diatom and *P. pouchetii* biomass show strong dependences on both absolute nutrient levels and *N* residual (Fig. 8b), a pattern very much similar to the observed (Fig. 4b).

3.3. MB nutrient sources

The GOM intruding flow transports nutrients and biota from the western GOM coast into MB through the North Passage (Jiang et al., 2007b,c). A first-order estimate based on historical and model data suggests that the intruding flow supplies the overwhelming bulk of the nutrient flux to MB with additional input from local sources including the MWRA effluent and atmospheric deposition (Table 1). This is generally consistent with an earlier estimate by HyroQual and Normandeau (1995). Thus, processes responsible for the nutrients and phytoplankton upstream of MB (Fig. 1) may be critically important to MB phytoplankton blooms. This is a dynamic area receiving the combined freshwater input from several local rivers (Saco, Kennebec, and Penobscot Rivers), mixing of Maine deep waters, as well as input from the EMCC (Brooks, 1985; Lynch et al., 1997; Pettigrew et al., 2005).

The coastal currents in the western GOM carry waters from river discharges and deeper offshore GOM waters. The intermediate depth waters in the GOM (50–150 m) are influenced by winter convective mixing (Brown and Irish, 1993; Hopkins and Garfield, 1979) and inputs

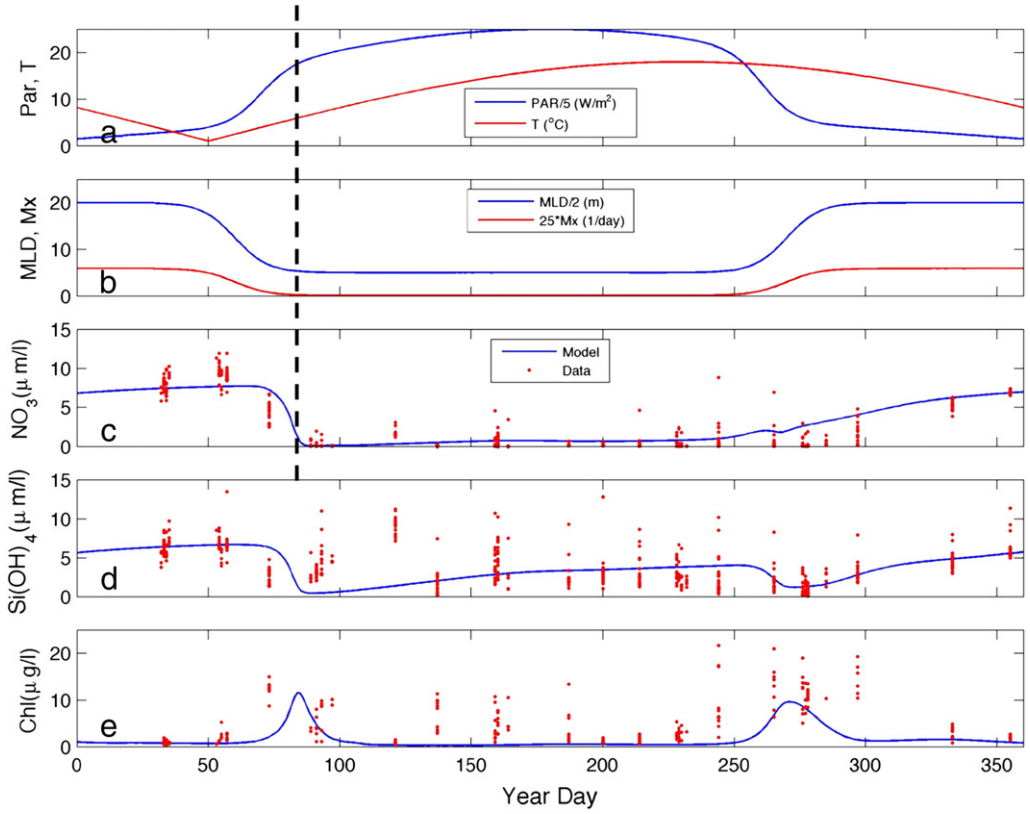

Fig. 5. 0-D model results and observed surface nutrient and chlorophyll in western MB initialized with 2000 winter nutrient concentrations: (a) PAR and temperature, (b) mixed layer depth and vertical mixing across mixed layer; (c) modeled and observed nitrate in 2000, (d) modeled and observed silicate in 2000; (e) model and observed chlorophyll in 2000.

of fresh and cold Scotian Shelf waters, the transport of which may be increasing in recent decades as a result of increased freshwater fluxes from upstream of Scotian Shelf (Ji et al., 2008; Townsend et al., 2010). In the western Gulf of Maine, the intermediate depth waters have relatively higher nitrate than silicate (Fig. 9a). Vertical mixing by winds and convection during winter storms may mix those waters into the surface layer, leading to not only higher nutrient concentrations but also higher nitrogen residual at the surface layer.

River discharge also provides significant nutrient input directly to the surface layer with strongest inputs during spring freshets in the western GOM (e.g. Anderson et al., 2005). Along the GOM coast, river nutrients have much higher silicate than nitrate (Si/N = 2–6, Fig. 9b; Anderson et al., 2008; Hunt et al., 2005), in contrast to the GOM deep waters.

Pre-bloom nutrient measurements at the MB entrance (stations F26–F28) suggest that river discharges and winter deep mixing have strong impacts on the nutrient characteristics of the MB intruding flow (Fig. 10). In particular, the nitrate residual (silicate deficit) has increased significantly in the last 15 years at a time when *P. pouchetii* blooms appear to have increased (Fig. 3a). This shift to a silicate deficit coincides with a period of strengthening surface wind speeds, possibly in response to intensifying storm activities (Fig. 10). For example, most of the strong *P. pouchetii* years since 2000, except 2008, experienced strong winter winds, and low Merrimack River flow. Furthermore, the N residual is significantly correlated with both winter surface winds and river flow.

4. Discussion

4.1. Phytoplankton resource competition

In this section, we discuss the model and observation results through the context of resource competition (Tilman, 1977, 1982). These results are generally consistent with the so-called *r*-selection strategy, which predicts that species with fastest growth (*r*-specialist) would dominate in a variable environment with high but patchy nutrient fluxes (Kilham and Hecky, 1988; McArthur and Wilson, 1967; Turpin and Harrison, 1979). Previous *Phaeocystis* studies have largely focused on the 'silicate hypothesis', in which diatoms outgrow *Phaeocystis* until silicate become limiting (Lancelot et al., 1987), suggesting the importance of N/Si ratio (e.g., Turner et al., 1998). However, silicate depletion is not a necessary condition for a *Phaeocystis* bloom. Since diatoms take up both nitrate and silicate with a nearly 1:1 molecular ratio, an earlier diatom bloom will consume most of the nitrate if the pre-bloom nitrate is less than silicate. In contrast, when nitrate is higher than silicate, diatom growth will be limited by silicate and the residual nitrogen will allow non-siliceous species to grow. On the other hand, if the both initial N and Si are sufficiently high, diatoms will take more time to consume the available nitrate, which may allow non-diatom species to grow significantly even if winter nitrate is lower than silicate. This suggests the importance of both absolute value of nutrients and N residual, as demonstrated by the high percentage (65%) of *P. pouchetii* abundance variance explained by the nitrate and residual nitrogen combined through a two-way ANOVA analysis.

Phaeocystis blooms under high nitrate and silicate situations may be further explained by considering the biomass equations of two species (P_1 for diatoms and P_2 for *Phaeocystis*) competing for nitrogen (N),

$$\begin{aligned}\rho_1 &\equiv \frac{1}{P_1}\frac{dP_1}{dt} = \mu_1 \frac{N}{k_1 + N} - m_1 \\ \rho_2 &\equiv \frac{1}{P_2}\frac{dP_2}{dt} = \mu_2 \frac{N}{k_2 + N} - m_2\end{aligned} \tag{8}$$

where ρ_i, μ_i, k_i, and m_i ($i = 1, 2$) represent the net growth, maximum growth, half-saturation constant, and mortality rate, respectively. The mortality rate includes natural death, sinking and grazing loss. For

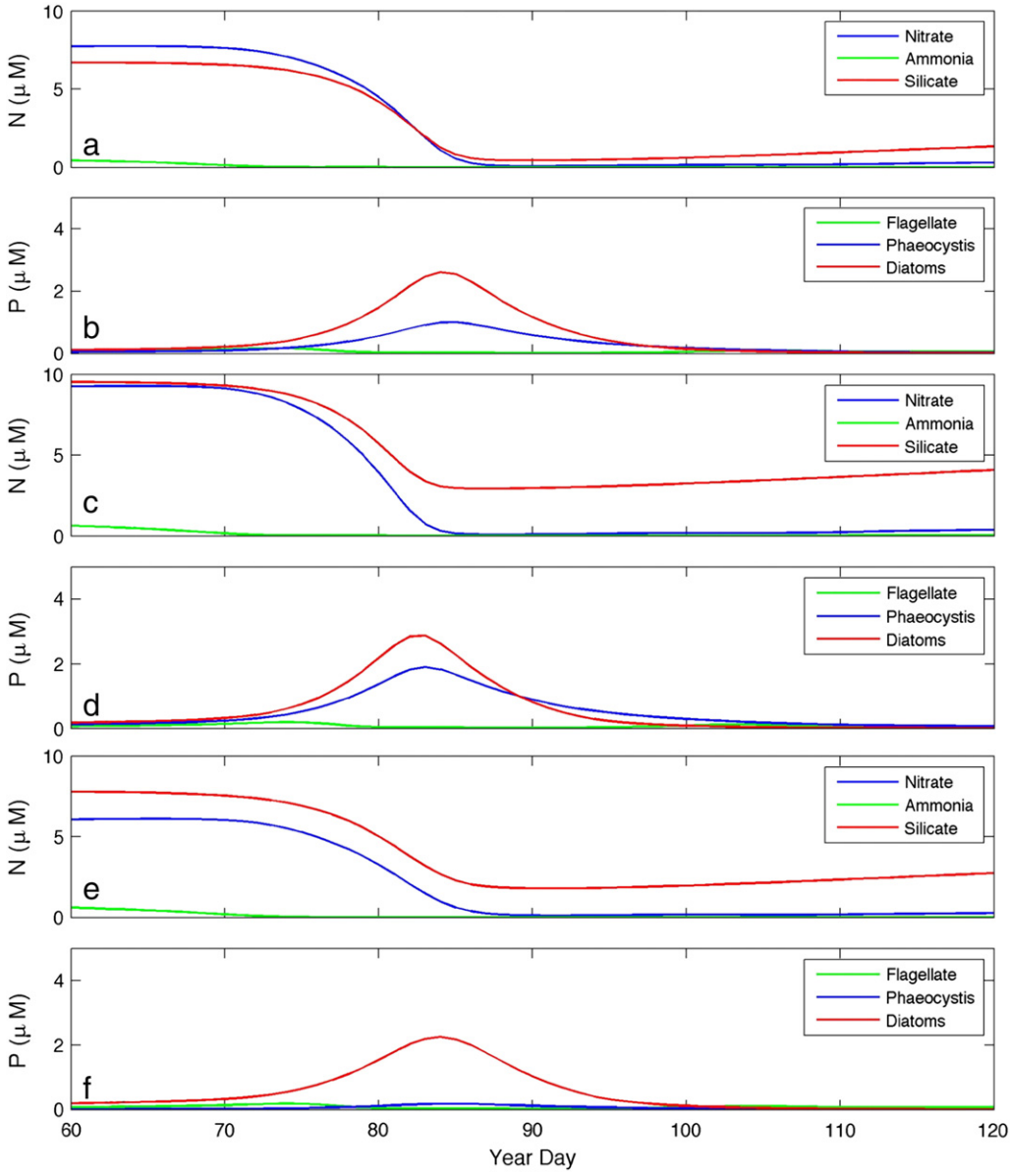

Fig. 6. Model nutrient concentrations and phytoplankton biomass: (a) and (b) 2000, (c) and (d) 2004, and (e) and (f) 1995. Only results in the spring bloom period are shown to highlight the competition between diatoms and *P. pouchetii*. Same physical forcing parameters are applied to the simulations (see Fig. 5a and 5b).

simplicity, we assume that $k_1 = k_2 = k$. Then the critical nutrient concentration when the two species grow at the same rate is,

$$N_c = k\frac{\delta m}{\delta\mu - \delta m} \tag{9}$$

where $\delta m = m_1 - m_2$, $\delta\mu = \mu_1 - \mu_2$. Diatoms typically grow faster than *Phaeocystis* and if we assume light is not limiting then $\delta\mu$ is a fixed positive value. During the initial development of the spring bloom, δm is small and hence *Nc* is small. Therefore, diatoms will generally grow faster. However, a sufficient high pre-bloom (winter) *N* will allow diatoms to keep growing long enough without exhausting the nutrient, which will allow zooplankton populations to respond. As a result, zooplankton grazing will become important in the later stage of the bloom development. Because *Phaeocystis* colonies can mostly escape grazing (low mortality as compared to diatoms), δm increases rapidly and hence *Nc* increases rapidly as well. At the same time, nitrate is being consumed and decreases rapidly. At some point, available nitrate will be lower than *Nc*, and *Phaeocystis* will start to grow faster than diatoms, either co-blooming with or out-competing diatoms. This scenario is consistent with the modeled bloom development during high winter N years (e.g., 2004 and 2007) (Fig. 6a and b).

Our results are also consistent with many other studies in mid- or high- latitude regions, which have shown that diatoms and *Phaeocystis* compete for nutrients (e.g. Egge and Aksnes, 1992; Lancelot and Rousseau, 1994; and Officer and Ryther, 1980). In the Southern Ocean, where light has been an important limiting factor to phytoplankton growth (Nelson and Smith, 1991), it has been suggested that the light and stratification conditions are critical in regulating the dominances between diatoms and *Phaeocystis* (Arrigo et al., 1999, 2003). However, a field study in Belgian coastal waters suggests that annual variation in irradiance is a greater factor in explaining winter–spring diatom abundance variability than *Phaeocystis* bloom variability (Gypens et al., 2007). Consistent with this, experimental evidence using MB

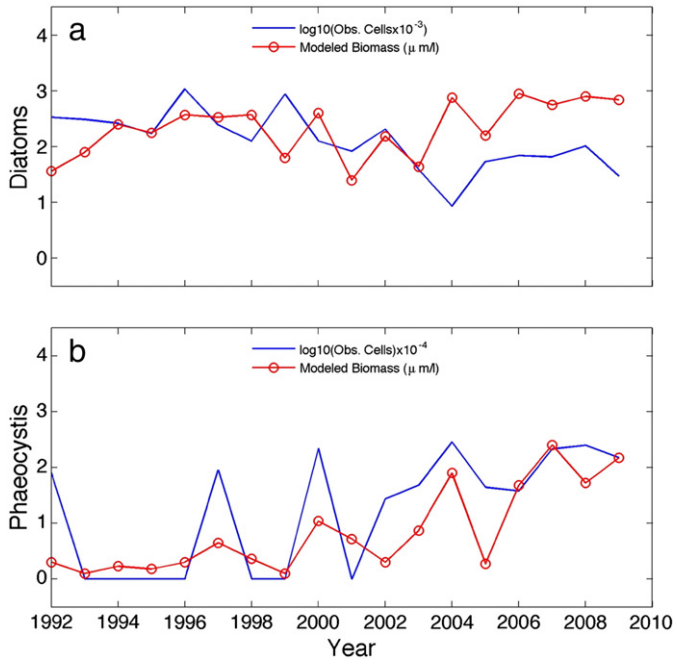

Fig. 7. Maximum biomass of modeled diatoms and *P. pouchetii* versus observed mean cell counts of observed diatoms and *P. pouchetii* in March–April period: (a) diatoms and (b) *P. pouchetii*. Note the observed cell counts are shifted to scale. Modeled maximum diatom biomass is not significantly correlated with observed diatom cell counts ($r = 0.3$, $p = 0.1$). However, modeled *P. pouchetii* maximum biomass is significantly correlated with observed cell counts ($r = 0.71$, $p < 0.01$).

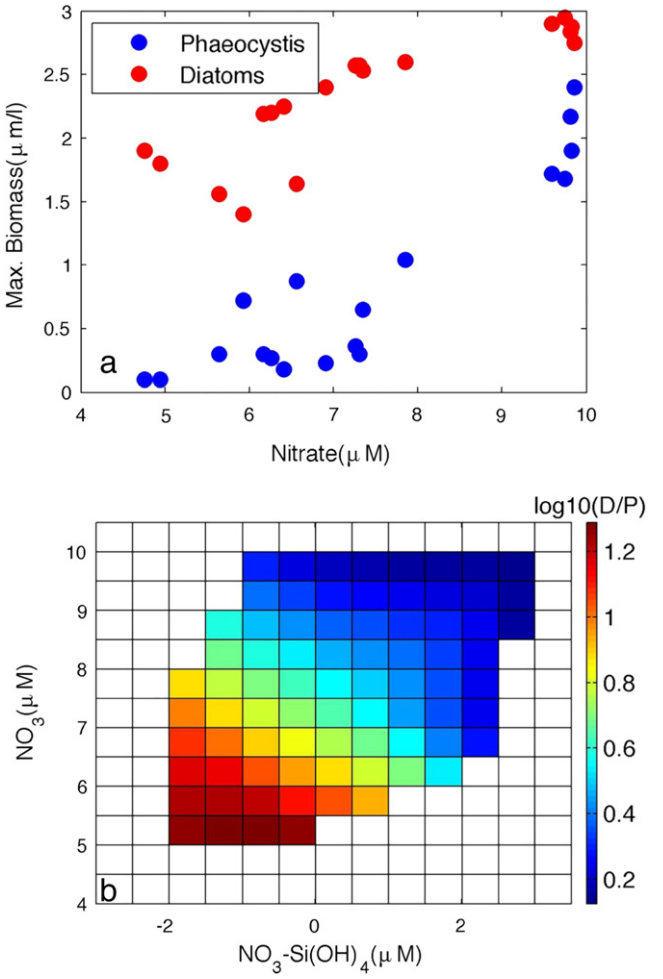

Fig. 8. (a) Modeled maximum diatom and *P. pouchetii* biomass during the spring bloom versus winter (initial) nitrate concentrations. (b) Relative peak biomass of diatom and *P. pouchetii* (log10(diatom/Phaeo)) in spring blooms versus nitrate and N residual from 18 model simulations for each year of 1992–2009. *P. pouchetii* biomass is assigned a low value 0.1 when the modeled biomass is less than 0.1 μmol N/l.

P. pouchetii clones suggests that its ability to compete with diatoms is also sensitive to irradiance levels (Hegarty and Villareal, 1998). Thus the magnitudes of *Phaeocystis* blooms may be further modulated by variation in irradiance, in addition to their dependence on pre-bloom nutrients shown in our analysis. While not explored in our model, the role of N to P ratio may also influence *P. pouchetii* bloom magnitude in MB. An integrated river-ocean model has suggested that an N to P ratio of >25 is a threshold for dominance of *Phaeocystis* over diatoms in Belgian coastal water (Lancelot et al., 2007, 2009).

4.2. External forcing

The GOM intruding flow is a mixture of fresher coastal waters through a coastal plume and the GOM deep waters through the WMCC (Fig. 1). The different nutrient characteristics between river input and GOM deep waters suggest that the relative proportions of these two sources are critical to the actual nutrient characteristics in the intruding flow, which would in turn determine the pre-bloom nutrient conditions in MB. Analyses have shown that surface salinities in western MB during the Feb.–Mar. period were significantly higher during *P. pouchetii* bloom years than during non-bloom years (32.25 vs 31.76; Libby et al., 2008), suggesting that more GOM deep water (higher N residual) would favor *P. pouchetii* blooms. Surface winds and convection mixing by major storms mix GOM deep waters into the surface layer and hence may lead to higher nutrient concentrations but also higher nitrogen residual at the surface layer. These processes are consistent with the correlations seen between surface winds, river discharge and N residual measured at the MB entrance (Fig. 10). Recent studies have suggested that storm activities on the east coast of North America have increased over the last several decades (Chang, 2007 and references therein). As a result, it is likely that more deep water nutrients are being mixed with surface waters, which would tend to increase surface N residual. As the origin of WMCC and a meeting place of two main driving processes (river discharges and winter mixing), we hypothesize that the MB upstream (red box in Fig. 1) is likely the key area for understanding the external influences on MB spring blooms.

In addition to nutrient dynamics, the intruding inflow to MB transports phytoplankton populations from upstream. It is believed that *Alexandrium fundyense* cells transported from New Hampshire and Maine coastal waters have triggered several major red-tide blooms in MB in recent years (Anderson et al., 2005; Franks and Anderson, 1992a,b). Significant inter-annual and long-term variability in GOM phytoplankton abundances and species composition have been reported (Barton et al., 2003), which may in turn affect phytoplankton abundances and species composition in MB. While *P. pouchetii* blooms in the GOM deep waters generally occur later in the year (May–June) than in MB (March–April), Continuous Plankton Recorder data from the GOM also show a dramatic increase in *P. pouchetii* abundances since 1990s (J. Hare, NOAA, *pers. comm.*). This suggests that the increasing and intensifying *P. pouchetii* blooms are likely a GOM-wide phenomenon.

4.3. Influences of large-scale processes

The importance of GOM deep waters suggests that larger-scale processes may indirectly influence the MB system. Nutrients in the GOM deep waters are largely controlled by the inflow of North Atlantic slope waters through the Northeast Channel, which includes

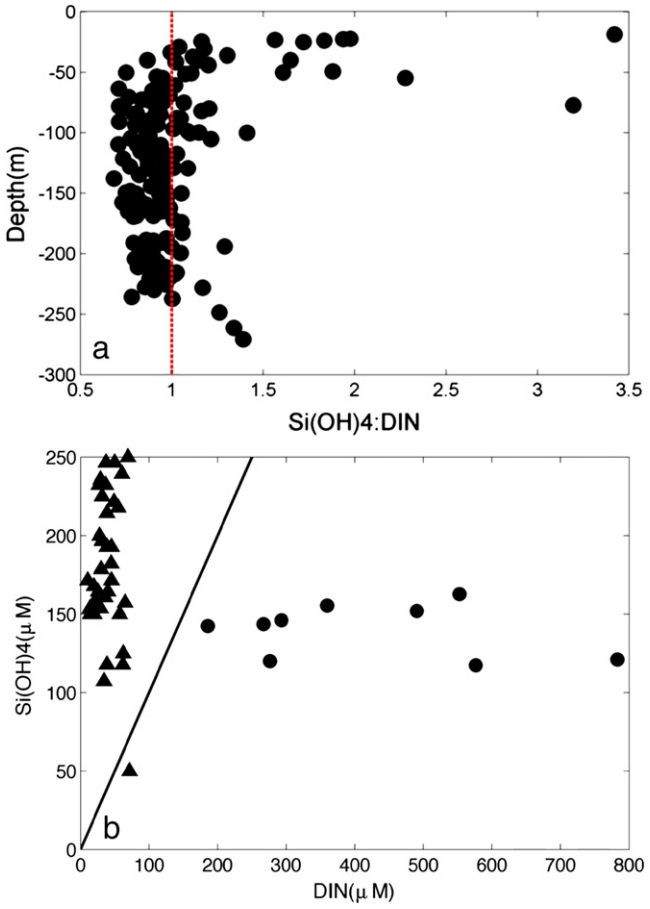

Fig. 9. (a) $Si(OH)_4$:DIN ratio versus water depth in GOM waters along northern coast measured in April 24–May 3, 2000. Red line indicates 1:1 ratio. (b) $Si(OH)_4$ versus DIN concentrations in Merrimack River during 1998–2001 (triangles) and MWRA effluent in 1995 (dots) (Effluent concentrations were divided by 3 to scale). Solid line indicates the 1:1 relationship between $Si(OH)_4$ and DIN.

contributions from Warm Slope Water (WSW) and cold Labrador Slope Water (LSW) (Petrie and Drinkwater, 1993; Ramp et al., 1985). The WSW carries higher nitrate (>23 μM) than LSW (ca. 15–16 μM) but has similar silicate (~10–14 μM; Townsend and Ellis, 2010). It is generally believed that the proportion of WSW and LSW varies in response to the North Atlantic Oscillations (NAO), with more WSW during positive NAO winter index years and vice versa. At intermediate depths, waters are dominated by the input of fresh and cold waters via the Grand Banks and the Scotian Shelf, which have been increasingly influenced in recent decades by freshwater input upstream of Scotian Shelf including Gulf of St. Lawrence and the Arctic melting (Ji et al., 2008; Townsend et al., 2010). Recently, Townsend et al. (2010) analyzed GOM long-term nutrient data (http://grampus.umeoce.maine.edu/nutrients/) and found significant long-term declines in nutrients at both intermediate and deep waters in the eastern GOM. They further argued that the enhanced Arctic melting has increased water and nutrient input into the GOM through the inner limb of Labrador Current water, whereas local nitrate losses through sediment denitrification and silicate accumulations through river discharges and in-situ regeneration may have contributed to changing nutrient regime.

Large-scale processes may also affect the regional meteorological processes such as winds and heat fluxes, and land-based processes such as river discharges (Dickson et al., 1996), which will in turn affect the coastal circulation and nutrient delivery. For example, it has been reported that the N-S component of surface winds or absolute wind speed measured at buoy 44013 in MB is significantly correlated with the winter NAO index (Jiang et al., 2007a; Turner et al., 2006). The winter storm activity in the eastern coast of United States also has increased significantly since 1950 (Chang, 2007; also see http://ecws.eas.cornell.edu), which in turn will affect winter mixing in the GOM. The increase of storm activity appears to have aligned well with the increase of NAO index since 1960 until 2010. On the other hand, enhanced Arctic melting may also affect the vertical stratification in the GOM, partly offsetting the storm mixing effects.

The impacts of NAO on the regional stream flow remain unclear. A recent study by Tootle et al. (2005) found no significant influences of NAO on stream flow in the northeast US using data for the period 1951–2002. However, a simple analysis of winter flow from Merrimack River in 1950–2010 indicates that it is positively correlated with the winter NAO index (Fig. 11). This suggests that the NAO may have disproportionally affected stream flow in the GOM coastal region. This is consistent with research findings in Belgian coastal waters where *Phaeocystis* bloom variability is largely driven by oceanographic- and meteorological-driven variations in nutrient delivery. Moreover, the competition between diatoms and *Phaeocystis* in Belgian coastal waters is determined by a non-linear relationship between NAO and riverine input of nitrate, with elevated nitrate concentration and *Phaeocystis* abundance during negative NAO periods (Breton et al., 2006).

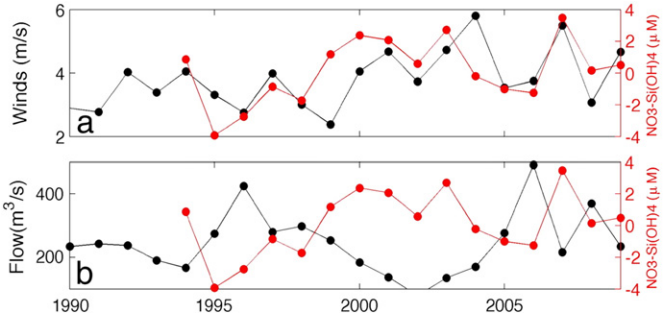

Fig. 10. (a) Surface wind speed (Jan.–Feb.) at NDBC 44013 and N residual (NO_3–$Si(OH)_4$) at stations F26–28 in February ($r = 0.54$, $p < 0.05$). Wind data at 44013 were suspicious during February 2001 and 2006, and data from a nearby station IOSN3 (off NH coast) were used instead. (b) Merrimack River discharge (Jan.-Feb.) and nitrate residual at stations F26–28 ($r = -0.62$ $p < 0.05$). Because usually there was only one (mid-February) MWRA cruise along the open boundary before the spring bloom, March flow and wind data are not included.

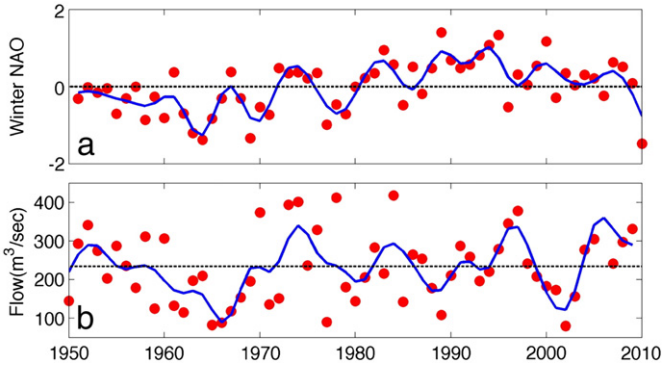

Fig. 11. (a) Winter (December–March) NAO index computed from NCEP re-analysis products (http://www.cpc.ncep.noaa.gov/data/teledoc/nao.shtml), and (b) winter (December–February) Merrimack River flow. Blue lines are low-pass filtered with a Lanczos filter with a cut off period of 5 years. The correlation coefficient between the two indices is $r = 0.37$ ($p < 0.01$).

5. Conclusions

An analysis of long-term observations in MB over the last two-decades (1992–2010) indicates that there were strong inter-annual variability and possibly long-term changes in the phytoplankton communities during the MB spring bloom. In particular, *P. pouchetii* blooms became more frequent with increasing abundances, whereas diatom abundances were in decline. Further analysis suggests that pre-bloom nutrient concentrations (equivalent to winter nutrients), both the absolute values and N residual, were critical in controlling the relative abundances between *P. pouchetii* and diatoms.

A new biogeochemical model was developed to explicitly simulate the competition between diatoms and *P. pouchetii* blooms during springtime in Massachusetts Bay. A series of idealized two-layer 0-D numerical simulations were carried out using the same idealized physical forcing but variable winter nutrients (based on observations) for each year between 1992 and 2009. Modeled phytoplankton biomass during the spring bloom periods were analyzed along with the observed phytoplankton abundances during the same periods in relation to the pre-bloom nutrients. Modeled results were generally consistent with the observed *P. pouchetii* and diatom variations during 1992–2010. Moreover, modeled results and the data analysis indicate the important role of winter nutrients in the competition between these two phytoplankton groups during the MB spring bloom, consistent with the resource competition theory in that species with fastest growth (so-called *r*-specialist) would dominate in a variable environment (e.g. Tilman, 1982). However, if winter nutrient concentrations are sufficiently high, both species may grow substantially even though diatoms remain to be the *r*-specialist and bloom first.

The reasons of observed nutrient variations in Massachusetts Bay were investigated using observed February nutrient concentrations at three boundary stations during 1992–2009, winter Merrimack River discharges, and winter surface winds in MB. The results indicate that the MB nutrient input is significantly correlated with both river discharges and surface winds in the western Gulf of Maine region. While the river effect is relatively obvious, the wind effect is likely due to the winter convective mixing, which brings nutrients from the GOM deep waters to the surface and subsequently into MB through coastal transport. Moreover, both river discharges and convective mixing processes may have been regulated by large-scale processes such as Arctic melting and North Atlantic Oscillations through hydrological cycle, meteorological forcing, and regional circulation.

Acknowledgments

This work is partly supported by the Massachusetts Water Resources Authority and University of Massachusetts Boston Healey Endowment Grant. We thank continuous encouragement and discussion from Dr. M. Mickelson at MWRA. Two anonymous reviewers' comments greatly improved this manuscript.

Appendix A. Model equations

A.1. Nutrients

In this simple model, nitrogen is equivalent to carbon through a fixed Redfield carbon to nitrogen ratio. Therefore, nitrogen uptake is equivalent to phytoplankton growth. The second assumption is that we ignore the mixing effect through the thermocline on the phytoplankton and zooplankton. For a horizontally uniform problem (0-D assumption), Eq. (1) is simplified as follows,

$$dN/dt = \frac{\partial}{\partial z}\left(k_z \frac{\partial N}{\partial z}\right) + \text{sources} - \text{sinks} \tag{A1}$$

where z is the vertical coordinate and k_z is the vertical mixing coefficient. Integrating and averaging A1 over the surface mixed layer, we have,

$$d\overline{N}/dt = -\left(k_z \frac{\partial N}{\partial z}\right)|_{z=-mld}/mld + (\text{sources} - \text{sinks})/mld \tag{A2}$$

where *mld* is the surface mixed layer depth. Here we have taken into account that there are no tracer fluxes at the sea surface ($z = 0$). Assuming the thickness of the thermocline as δh, A2 can be written as follows,

$$d\overline{N}/dt = m_x(N_l - \overline{N}) + (\text{sources} - \text{sinks})/mld \tag{A3}$$

where N_l represents the tracer value at the lower layer and $m_x = k_z(z = -mld)/(\delta h * mld)$. A similar equation can be derived for tracers in the lower layer. Similar equations have been used by Evans and Parslow (1985) and Fasham et al. (1990).

Therefore, the model equations for nutrients can be written as following,

$$\begin{cases} \dfrac{d\mathrm{NO_3}}{dt} = -\displaystyle\sum_{k=1}^{3} uptake_k^{\mathrm{NO3}} + m_{nh4}\mathrm{NH4}Q_d + m_x(\mathrm{NO3}_l - \mathrm{NO3}) \\ \dfrac{d\mathrm{NH_4}}{dt} = -\displaystyle\sum_{k=1}^{3} uptake_k^{\mathrm{NH4}} + \sum_{l=1}^{2} exc_l Z_l Q_z + m_d DQ_d - m_{nh4}\mathrm{NH4}Q_d \\ \qquad\qquad + \displaystyle\sum_{k=1}^{3} resp_k + m_x(\mathrm{NH4}_l - \mathrm{NH4}) \\ \dfrac{d\mathrm{SiO_4}}{dt} = -uptake^{\mathrm{Si(OH)_4}} + m_{bsi}BSiQ_d + m_x(\mathrm{Si(OH)_4} - \mathrm{Si(OH)_4}) \end{cases} \tag{A4}$$

Nutrient uptakes include three factors: light, nutrient, and temperature (so-called Q10 effect). All three phytoplankton uptake nitrogen,

$$\begin{cases} uptake_k^{\mathrm{NO3}} = f_k(I)g_k(T)\mu_k^{\mathrm{NO3}}P_k \\ uptake_k^{\mathrm{NH4}} = f_k(I)g_k(T)\mu_k^{\mathrm{NH4}}P_k \end{cases} \quad \mathrm{k} = 1, 2, 3. \tag{A5}$$

For microflagellate and *P. pouchetii*,

$$\begin{cases} \mu_k^{\mathrm{NO3}} = V_m^k \dfrac{e^{-\psi_k \mathrm{HH4}}\mathrm{NO_3}}{K_{no3}^k + \mathrm{NO_3}} \\ \mu_k^{\mathrm{NH4}} = V_m^k \dfrac{\mathrm{NH_4}}{K_{nh4}^k + NH4} \end{cases} \qquad \mathrm{k} = 1, 2. \tag{A6}$$

Silicate uptake is solely due to diatoms,

$$uptake^{\mathrm{Si(OH)_4}} = f_3(I)g_3(T)\mu_3^{\mathrm{Si(OH)_4}}P_3. \tag{A7}$$

In coastal environment, both dissolved inorganic nitrogen and silicate are generally replete during winter and early spring bloom. Therefore, we assume the diatoms are under healthy growth condition and so the uptakes of nitrogen and silicate follow N/Si = 1 ratio,

$$\mu_3^{\mathrm{NO3}} + \mu_3^{\mathrm{NH4}} = \mu_3^{\mathrm{Si(OH)_4}} = \mu_3. \tag{A8}$$

The uptake is co-limited by nitrogen and silicate, which follows the Liebig's Law,

$$\mu_3 = V_m^3 \min\left(\left(\frac{e^{-\psi_3 \mathrm{NH4}}\mathrm{NO_3}}{K_{no3}^3 + \mathrm{NO_3}} + \frac{\mathrm{NH_4}}{K_{nh4}^3 + \mathrm{NH_4}}\right), \ \frac{\mathrm{Si(OH)_4}}{K_{\mathrm{Si(OH)_4}}^3 + \mathrm{Si(OH)_4}}\right). \tag{A9}$$

Therefore,

$$\begin{cases} \mu_3^{NO_3} = \mu_3 \dfrac{a^{NO_3}}{a^{NO_3} + a^{NH_4}} \\ \mu_3^{NH_4} = \mu_3 \dfrac{a^{NH_4}}{a^{NO_3} + a^{NH_4}} \end{cases} \tag{A10}$$

where $a^{NO_3} = \frac{e^{-\psi_3 NH_4} NO_3}{K^3_{NO_3} + NO_3}$, $a^{NH_4} = \frac{NH_4}{K^3_{NH_4} + NH_4}$.

Limited research data on *P. pouchetii* half-saturation uptake values suggested that the colonial cells have much higher (up to 8 times) half-saturation concentrations (for both N and P) than free living cells (Schoemann et al., 2005; Veldhuis et al., 1991; also see model parameters chosen by Lancelot et al., 2005). But *P. pouchetii* colonies are generally considered not limited by P because their capability using organic P (Veldhuis et al., 1991).

The respiration terms ($resp_k$) represent the collective effects of phytoplankton respiration and exudation, which is formulated as a fixed percentage of primary production,

$$resp_k = r_P^k \left(\mu_k^{NO_3} + \mu_k^{NH_4} \right) \quad k = 1, 2, 3. \tag{A11}$$

A.2. Phytoplankton

$$\begin{aligned} \frac{dP_k}{dt} = {} & \mu_k^{NO_3} + \mu_k^{NH_4} + \delta_{k1} p1p2 + \delta_{k2} p2p1 - graz_{pk} - resp_k \\ & - S_P^k P_k / mld - m_P^k P_k Q_p \quad k = 1, 2, 3 \end{aligned} \tag{A12}$$

where $\delta_{11} = -1$, $\delta_{12} = 1$, $\delta_{21} = 1$, and $\delta_{22} = -1$. Here we ignore the entrainment effect of mixed layer deepening on phytoplankton, which mainly occurs during fall blooms and storm events. This is because we mainly focus on the spring bloom.

For microflagellate and *P. pouchetii*, nitrogen uptake is defined in Eq. (A6). For diatoms (P3), μ_k is co-limited by nitrogen and silicate as defined in Eqs. (A9) and (A10).

The terms p1p2 and p2p1 represent the aggregation of microflagellate to *P. pouchetii* and disruption of *P. pouchetii*, respectively,

$$\begin{cases} \text{p1p2} = 0 \\ \text{p2p1} = lycol * (1 - aggr) * \text{p2} \end{cases} \tag{A13}$$

where aggr represent the detrital portion of lysis *P. pouchetii* colonies. In our study, p1p2 is set to as zero following Lancelot et al. (2005).

A.3. Zooplankton

$$\begin{cases} \dfrac{dZ_1}{dt} = \gamma_1 graz_1 - graz_{zz} - exc_1 Z_1 Q_z - m_z^1 Z_1 Q_z \\ \dfrac{dZ_2}{dt} = \gamma_2 graz_2 - exc_2 Z_2 * Q_z - m_z^2 Z_2^2 Q_z \end{cases} \tag{A14}$$

where total grazing by meso-zooplankton (Z_2) is the combination of three prey,

$$graz_2 = graz_{p2} + graz_{p3} + graz_{zz}. \tag{A15}$$

Grazing follows the third Hollings-type formulation. Microflagellate are grazed upon by micro-zooplankton,

$$graz_1 = R_m^1 Z_1 \frac{P_1^2}{k_{z1}^2 + P_1^2} Q_z. \tag{A16}$$

P. pouchetii and diatoms both are grazed upon by meso-zooplankton, which is determined by the overall food availability and the grazing preference,

$$graz_{pk} = R_m^2 f_{pk}^{pre} \frac{P_k^2}{k_{z2}^2 + f_{z1}^{pre} Z_1^2 + f_{p2}^{pre} P_2^2 + f_{p3}^{pre} P_3^2} Z_2 Q_z \quad k = 2, 3 \tag{A17}$$

$$graz_{zz} = R_m^2 f_{z1}^{pre} \frac{Z_1^2}{k_{z2}^2 + f_{z1}^{pre} Z_1^2 + f_{p2}^{pre} P_2^2 + f_{p3}^{pre} P_3^2} Z_2 Q_z. \tag{A18}$$

A.4. Organic matter and biogenic silica

In this simplified version, detritus includes all types of organic materials (labile or refractory, dissolved or particulate). The equation is as follows,

$$\begin{aligned} \frac{dD}{dt} = {} & \sum_{k=1}^{3} m_p^k P_k Q_p + \sum_{l=1}^{2} (1 - \gamma_l) graz_l + \left(m_z^1 Z_1 + m_z^2 Z_2^2 \right) Q_z - S_d D / mld - m_d D Q_d \\ & + lycol * aggr * P2. \end{aligned} \tag{A19}$$

The biogenic silica derived from phytoplankton mortality and meso-zooplankton grazing,

$$\frac{dBSi}{dt} = m_p^3 P_3 Q_p + graz_{p3} - S_{bsi} BSi / mld - m_{bsi} BSi Q_d. \tag{A20}$$

In A20 the grazing consumption of diatoms by meso-zooplankton is pooled to BSi pool directly as meso-zooplankton don't store silica.

A.5. Lower layer processes

The lower layer is assumed to be deep enough such that any phytoplankton is well mixed and cannot grow. Therefore any phytoplankton in lower layer will be pooled into detritus pool immediately. Zooplankton is assumed to be able to maintain their depth without being mixed to the lower layer.

$$\begin{cases} \dfrac{\text{dNO3}_l}{dt} = +m_{nh4}^l \text{NH4}_l Q_d + m_x (\text{NO3} - \text{NO3}_l) \\ \dfrac{\text{dH4}_l}{dt} = -m_{nh4}^l \text{NH4}_l Q_d + m_x (\text{NH4} - \text{NH4}_l) + m_D^l D_l Q_d \\ \dfrac{\text{dSiO4}_l}{dt} = +m_{bsi}^l BSi_l Q_d + m_x (\text{Si(OH)}_4 - \text{Si(OH)}_4) \\ \dfrac{dD_l}{dt} = +S_D D / mld + \sum_{k=1}^{3} S_p^k P_k / mld - m_D^l D_l Q_d \\ \dfrac{dBSi_l}{dt} = +S_{bsi} BSi / mld + S_P^3 P_3 / mld - m_{bsi}^l BSi_l Q_d \end{cases} \tag{A21}$$

A.6. Light, temperature and mixing

All phytoplankton, zooplankton and detritus related process rates change along with the ambient temperature (Q_{10} effect), which is defined as,

$$\begin{cases} Q_p = \exp\left(a_{10p} \left(T - T_{ref} \right) \right) \\ Q_z = \exp\left(a_{10z} \left(T - T_{ref} \right) \right) \\ Q_d = \exp\left(a_{10d} \left(T - T_{ref} \right) \right) \end{cases}. \tag{A22}$$

The light acclimation $f(I)$ is the photosynthetic rate of phytoplankton, which is defined as (Platt et al., 1980),

$$f_k(I) = \left(1-\exp\left(-\alpha_k \bar{I}/V_m^k\right)\right)\exp\left(-\beta_k \bar{I}/V_m^k\right) \qquad k = 1,2,3 \tag{A23}$$

where $\bar{I}$ is mean PAR within the surface mixed layer,

$$\bar{I} = \frac{I}{k_{ext} mld} \tag{A24}$$

where *mld* is the mixed layer depth defined below.

The temperature dependence of phytoplankton growth takes the following form (Jiang et al., 2007b),

$$g_k(T) = \exp\left(-\left(T-T_{OPT}^k\right)^2/dT_k^2\right) \qquad k = 1,2,3. \tag{A25}$$

The optimal growth formulations are based on observed relationship between growth and temperature (Eppley, 1972; Schoemann et al., 2005).

The water temperature (T), solar radiation (I), mixed layer depth (*mld*), and vertical mixing (m_x) all change with season (we ignore the diurnal cycle). They are analytically specified as follows,

$$I = I_{\min} + (I_{\max} - I_{\min})\sin\left(\frac{\pi t}{360}\right) \tag{A26}$$

$$T = T_{\min} + (T_{\max} - T_{\min})\left|\sin\left(\frac{\pi(t-t_0)}{360}\right)\right| \tag{A27}$$

$$\begin{cases} m_x = m_{x0} + m_{x1} th(\eta_1(t-t_1)) & t \le 180 \\ m_x = m_{x0} + m_{x1} th(-\eta_2(t-t_2)) & t \ge 180 \end{cases} \tag{A28}$$

$$\begin{cases} mld = 0.5(mld_1 + mld_2) + 0.5(mld_2 - mld_1) th(\eta_1(t-t_1)) & t \le 180 \\ mld = 0.5(mld_1 + mld_2) + 0.5(mld_2 - mld_1) th(-\eta_2(t-t_2)) & t \ge 180 \end{cases} \tag{A29}$$

where t is the time in calendar day. The results of these empirical functions mimic the seasonal cycles of these parameters in the MB and Gulf of Maine region.

Appendix B. Model variables

NO_3 (μm/l)	1	Nitrate concentration at upper layer
NH_4 (μm/l)	2	Ammonia concentration at upper layer
SiO_4 (μm/l)	3	Silicate concentration at upper layer
p1 (μm/l)	4	Microflagellate biomass
p2 (μm/l)	5	*P. pouchetii* biomass
p3 (μm/l)	6	Diatom biomass
z_1 (μm/l)	7	*Micro*-zooplankton biomass
z_2 (μm/l)	8	*Meso*-zooplankton biomass
D (μm/l)	9	Detritus concentration
BSi (μm/l)	10	Biogenic silica concentration
NO_{3l} (μm/l)	11	Nitrate concentration at lower layer
NH_{4l} (μm/l)	12	Ammonia concentration at lower layer
SiO_{4l} (μm/l)	13	Silicate concentration at lower layer
Dl (μm/l)	14	Detritus concentration at lower layer
BSil (μm/l)	15	Biogenic silica concentration at lower layer
T (°C)		Water temperature
I (W/m^2)		Photosynthetically available radiation (PAR) at surface
m_x (1/day)		Vertical mixing coefficient across the thermocline
mld (m)		Mixed layer depth

Note prognostic variables are numbered, whereas other variables are pre-defined.

Appendix C. Model parameters

Value	Symbol (unit)	Descriptions	
1.3	V^1_m (day^{-1})	Max. microflagellate growth rate	[1,2]
1.8	V^2_m (day^{-1})	Max. *P. pouchetii* growth rate	[1]
2.5	V^3_m (day^{-1})	Max. diatom growth rate	[3,4]
0.2	$K^1_{NO_3}$ (μmol/l)	Half saturation for microflagellate nitrate uptake	
2.0	$K^2_{NO_3}$ (μmol/l)	Half saturation for *P. pouchetii* nitrate uptake	
3.0	$K^3_{NO_3}$ (μmol/l)	Half saturation for diatom nitrate uptake	[3]
0.05	$K^1_{NH_4}$ (μmol/l)	Half saturation for microflagellate ammonia uptake	
0.5	$K^2_{NH_4}$ (μmol/l)	Half saturation for *P. pouchetii* ammonia uptake	
0.5	$K^3_{NH_4}$(μmol/l)	Half saturation for diatom ammonia uptake	
3.0	$K^3_{Si(OH)_4}$ (μmol/l)	Half saturation for diatom silicate uptake	[3]
5	ψ1 ((μmol/l)$^{-1}$)	Ammonia inhibition for micro-flagellate nitrate uptake	
5	ψ2 ((μmol/l)$^{-1}$)	Ammonia inhibition for *P. pouchetii* nitrate uptake	
5	ψ3 ((μmol/l)$^{-1}$)	Ammonia inhibition for diatom nitrate uptake	

(continued on next page)

Appendix C (*continued*)

Value	Symbol (unit)	Descriptions	
0.02	m^1_p (day^{-1})	Micro-flagellate natural mortality rate	
0.05	m^2_p (day^{-1})	*P. pouchetii* natural mortality rate	
0.05	m^3_p (day^{-1})	Diatoms natural mortality rate	
0.1	r^1_p	Micro-flagellate respiration rate (percentage of PP)	[4]
0.1	r^2_p	*P. pouchetii* respiration rate (percentage of PP)	[4]
0.1	r^3_p	Diatom respiration rate (percentage of PP)	[4]
0.02	Lycol (day^{-1})	*P. pouchetii* lysis rate	
0.8	aggr	Detrital fraction of *P. pouchetii* lysis	
1.0	R^1_m (day^{-1})	Max. micro-zooplankton grazing rate	[5]
0.6	R^2_m (day^{-1})	Max. meso-zooplankton grazing rate	[6]
0.1	K^1_z (μmol/l)	Half saturation for micro-zooplankton grazing	
0.3	K^2_z (μmol/l)	Half saturation for meso-zooplankton grazing	
0.2	m^1_z (day^{-1})	Micro-zooplankton natural mortality rate	
0.2	m^2_z ($(day * \mu mol/l)^{-1}$)	Meso-zooplankton natural mortality rate	[7]
0.4	f^{pre}_{z1}	Meso-zooplankton grazing preference for micro-zoopl.	
0.02	f^{pre}_{p2}	Meso-zooplankton grazing preference for *P. pouchetii*	
0.58	f^{pre}_{p3}	Meso-zooplankton grazing preference for diatoms	
0.9	γ_1	Grazing efficiency for micro-zooplankton	[8]
0.7	γ_2	Grazing efficiency for meso-zooplankton	[8]
0.2	exc_1 (day^{-1})	Excretion rate for micro-zooplankton	
0.1	exc_2 (day^{-1})	Excretion rate for meso-zooplankton	
0.2	k_{ext} (m^{-1})	Light attenuation coefficient	[4]
0.0	S^1_p (m/day)	Micro-flagellate sinking velocity	
0.5	S^2_p (m/day)	*P. pouchetii* sinking velocity	[1]
1.5	S^3_p (m/day)	Diatom sinking velocity	[3]
10	S_d (m/day)	Sinking velocity of detritus	
10	S_{bsi} (m/day)	Sinking velocity of biogenic	
200	I_0 (W/m^2)	Daily mean photosynthetically available radiation	
0.025	α_1 ($(day * W/m^2)^{-1}$)	Initial slope of *P–I* curve for micro-flagellate	[4]
0.01	α_2 ($(day * W/m^2)^{-1}$)	Initial slope of *P–I* curve for *P. pouchetii*	
0.025	α_3 ($(day * W/m^2)^{-1}$)	Initial slope of *P–I* curve for diatoms	[4]
0.002	β_1 ($(day * W/m^2)^{-1}$)	Light inhibition parameter for micro-flagellate	
0.002	β_2 ($(day * W/m^2)^{-1}$)	Light inhibition parameter for *P. pouchetii*	
0.002	β_3 ($(day * W/m^2)^{-1}$)	Light inhibition parameter for diatoms	
0.01	m_D (day^{-1})	Detritus remineralization rate	
0.02	m_{BSi} (day^{-1})	Biogenic silica dissolution rate	
0.02	m_{nh4} (day^{-1})	Nitrification rate	
0.05	m^l_D (day^{-1})	Detritus remineralization rate at lower layer	
0.02	m^l_{BSi} (day^{-1})	Biogenic silica dissolution rate at lower layer	
0.05	m^l_{nh4} (day^{-1})	Nitrification rate at lower layer	
16	T_{OPT1} (°C)	Optimal temperature for micro-flagellate growth	[1]
12	T_{OPT2} (°C)	Optimal temperature for *P. pouchetii* growth	[1]
14	T_{OPT3} (°C)	Optimal temperature for diatoms growth	
13.7	dT_1 (°C)	STD of optimal temperature for micro-flagellate growth	[1]
13.7	dT_2 (°C)	STD of optimal temperature for *P. pouchetii* growth	[1]
12	dT_3 (°C)	STD of optimal temperature for diatoms growth	[3]
0.069	$a10_p$	Temperature dependence of phytoplankton processes (excl. sinking)	
0.1	$a10_z$	Temperature dependence of zooplankton processes	
0.12	$a10_d$	Temperature dependence of remineralization processes	
15	T_{ref} (°C)	Reference temperature for all processes	
0.12	m_{x0} (day^{-1})	Annual mean mixing coefficient between mixed layer and below	[9]
0.1	m_{x1} (day^{-1})	Difference of mixing coefficient in winter and summer	[10]
1.0	T_{min} (°C)	Minimum water temperature in winter	
18	T_{max} (°C)	Maximum water temperature in summer	
60	I_{min} (W/m^2)	Minimum daily mean PAR in winter	
250	I_{max} ($W/^2$)	Maximum daily mean PAR in summer	
0.08	η_1 (day^{-1})	Transition time scale of spring stratification	
0.08	η_2 (day^{-1})	Transition time scale of stratification collapse	
50	t_0 (day)	The date when water temperature reach minimum	
30	t_1 (day)	The date when stratification builds up	
240	t_2 (day)	The date when stratification collapses	
10	mld_1 (meter)	Minimum mixed layer depth	
40	mld_2 (meter)	Maximum mixed layer depth	

Note: Except explicitly stated, most parameters were modified from the BEM (Jiang et al., 2007b).
[1] Schoemann et al., 2005, [2] Hegarty and Villareal (1998), [3] Sarthou et al., 2005, [4] Jiang et al., 2007b, [5] Calbet and Landry (2004), scaled to phytoplankton growth rate 1.8 day^{-1}, [6] Calbet (2001), scaled to primary productivity at 2 gC/m^2/day, which is a typical value for Massachusetts Bay spring bloom (Oviatt et al., 2007). [7] Ohman et al. (2002), [8] Fasham et al. (1990) with adjustment. [9] Geyer and Ledwell (1997) reported a summer vertical mixing rate 0.06–0.18 cm^2/s near the thermocline in MB. Assuming $mld = 10$ m and $\delta h = 1$ m, $m_x = k_z/(\delta h * mld)$ is 0.5–0.15 day^{-1}. We chose a near upper end value. [10] Winter vertical mixing can 2 order higher than the summer value. But mld in MB is about 4–5 times deeper than summer mixed layer, and thermocline is likely much thicker as well. So m_x is likely about several times to an order higher than its summer value. We chose a rate about twice of the summer rate.

References

Anderson, D.M., Keafer, B.A., McGillicuddy, D.J., et al., 2005. Initial observations of the 2005 *Alexandrium fundyense* bloom in southern New England: general patterns and mechanisms. Deep-Sea Res. II 52, 2856–2876.

Anderson, D.M., Burkholder, J.M., Cochlan, W.P., et al., 2008. Harmful algal blooms and eutrophication: examining linkages from selected coastal regions of the United States. Harmful Algae 8 (1), 39–53.

Arrigo, K.R., Robinson, D.H., Worthen, D.L., et al., 1999. Phytoplankton community structure and the drawdown of nutrients and CO_2 in the Southern Ocean. Science 283, 365–367.

Arrigo, K.R., Worthen, D.L., Robinson, D.H., 2003. A coupled ocean-ecosystem model of the Ross Sea 2: iron regulation of phytoplankton taxonomic variability and primary production. J. Geophys. Res. 108 (C7), 3231. http://dx.doi.org/10.1029/2001JC000856.

Barton, A.D., Greene, C.H., Monger, B.C., Pershing, A.J., 2003. The Continuous Plankton Recorder survey and the North Atlantic Oscillation: interannual- to multidecadal-scale patterns of phytoplankton variability in the North Atlantic Ocean. Prog. Oceanogr. 58, 337–358.

Bigelow, H.B., 1927. Physical oceanography of the Gulf of Maine. Bull. U. S. Bur. Fish. 40 (Part II), 511–1027.

Breton, E., et al., 2006. Hydroclimatic modulation of diatom/phaeocystis blooms in nutrient-enriched Belgian coastal waters (North Sea). Limnol. Oceanogr. 51 (3), 1401–1409.

Brooks, D.A., 1985. Vernal circulation in the Gulf of Maine. J. Geophys. Res. 90, 4687–4705.

Brown, W.S., Irish, J.D., 1993. The annual variation of water mass structure in the Gulf of Maine: 1986–1987. J. Mar. Res. 51, 53–107.

Calbet, A., 2001. Mesozooplankton grazing effect on primary production: a global comparative analysis in marine ecosystems. Limnol. Oceanogr. 46 (7), 1824–1830.

Calbet, A., Landry, M.R., 2004. Phytoplankton growth, microzooplankton grazing, and carbon cycling in marine systems. Limnol. Oceanogr. 49 (1), 51–57.

Chang, E.K.M., 2007. Assessing the increasing trend in northern hemisphere winter storm track activity using surface ship observations and a statistical storm track model. J. Clim. 20, 5607–5628.

Churchill, J., Pettigrew, N.R., Signell, R.P., 2005. Structure and variability of the Western Maine Coastal Current. Deep-Sea Res. II 52, 2392–2410.

Dickson, R., Lazier, J., Meincke, J., Rhines, P., Swift, J., 1996. Long-term coordinated changes in the convective activity of the North Atlantic. Prog. Oceanogr. 38, 241–295.

Egge, J.K., Aksnes, D.L., 1992. Silicate as regulating nutrient in phytoplankton competition. Mar. Ecol. Prog. Ser. 83, 281–289.

Eilertsen, H.C., Raa, J., 1995. Toxins in seawater produced by a common phytoplankter: *Phaeocystis pouchetii*. J. Mar. Biotechnol. 3, 115–119.

Eppley, R.W., 1972. Temperature and phytoplankton growth in the sea. Fish. Bull. 70, 1063–1085.

Evans, G.T., Parslow, J.S., 1985. A model of annual plankton cycles. Biological Oceanography, vol. 3. Crane, Russak & Company, Inc., pp. 327–346.

Fasham, M.J.R., Ducklow, H.W., McKelvie, S.M., 1990. A nitrogen-based model of plankton dynamics in the oceanic mixed layer. J. Mar. Res. 48 (3), 591–639.

Franks, P.J.S., Anderson, D.M., 1992a. Alongshore transport of a toxic phytoplankton bloom in a buoyancy current: *Alexandrium tamarensis* in the Gulf of Maine. Mar. Biol. 112, 153–164.

Franks, P.J.S., Anderson, D.M., 1992b. Toxic phytoplankton blooms in the southwestern Gulf of Maine: testing hypotheses of physical control using historical data. Mar. Biol. 112, 165–174.

Geyer, R.W., Ledwell, J.R., 1997. Boundary Mixing in Massachusetts Bay. Massachusetts Water Resources Authority, Boston (Report 1997-09. 20 pp.).

Geyer, R.W., Gardner, G., Brown, W., et al., 1992. Physical oceanographic investigation of Massachusetts and Cape Cod Bays. Massachusetts Bay Program, MBP-92-03. Boston, Massachusetts (497 pp.).

Geyer, W.R., Signell, R.P., Fong, D.A., et al., 2004. The freshwater transport and dynamics of the western Maine coastal current. Cont. Shelf Res. 24, 1339–1357.

Gypens, N., Lacroix, G., Lancelot, C., 2007. Causes of variability in diatom and *Phaeocystis* blooms in Belgian coastal waters between 1989 and 2003: a model study. J. Sea Res. 57 (1), 19–35.

Hansen, E.E., Ernsten, H.C., Geneviere, A.-M., 2003. Anti-mitotic activity towards sea urchin embryos in extracts from the marine haptophycean *Phaeocystis pouchetii* (hariot) *Lagerheim* collected along the coast of northern Norway. Toxicon 41, 803–812.

Hegarty, S.G., Villareal, T.A., 1998. Effects of light level and N:P supply ratio on the competition between *Phaeocystis* cf. *pouchetii* (Hariot), Lagerheim (*Prymnesiophyceae*) and five diatom species. J. Exp. Mar. Biol. Ecol. 226, 241–258.

Hopkins, T.S., Garfield III, N., 1979. Gulf of Maine intermediate water. J. Mar. Res. 37, 103–139.

Hunt, C.D., West, D.E., Peven, C.S., 1995. Deer Island Effluent Characterization and Pilot Treatment Plant Studies: June 1993–November 1994. Massachusetts Water Resources Authority, Boston (Report 1995-07. 140 pp.).

Hunt, C.W., Loder, T., Vorsomarty, J., et al., 2005. Spatial and temporal patterns of inorganic nutrient concentrations in the Androscoggin and Kennebec Rivers, Maine. Water Air Soil Pollut. 163, 303–323.

Hunt, C.D., Borkman, D.G., Libby, P.S., et al., 2010. Phytoplankton Patterns in Massachusetts Bay—1992–2007. Estuar. Coasts 33 (2), 448–470. http://dx.doi.org/10.1007/s12237-008-9125-9.

HydroQual, Inc., Normandeau Associates, Inc., 1995. A Water Quality Model for Massachusetts and Cape Cod Bays: Calibration of the Bay Eutrophication Model (BEM). Massachusetts Water Resource Authority, Boston (Report 1995-08, 402 pp.).

Ji, R., et al., 2008. Modeling the influence of low-salinity water inflow on winter–spring phytoplankton dynamics in the Nova Scotian Shelf-Gulf of Maine region. J. Plankton Res. 30 (12), 1399–1416.

Jiang, M., Zhou, M., 2006a. The Massachusetts and Cape Cod Bays Hydrodynamic Model: 2002–2004 Simulation. Massachusetts Water Resources Authority, Boston (Report 2006-12. 128 pp.).

Jiang, M., Zhou, M., 2006b. Massachusetts Bay Eutrophication Model: 2002–2004 Simulation. Massachusetts Water Resources Authority, Boston (Report 2006-13. 126 pp.).

Jiang, M.S., Zhou, M., 2014. Dynamics of Gulf of Maine intruding current around Cape Ann, Massachusetts. Cont. Shelf Res. (to be submitted for publication).

Jiang, M., Brown, W.M., Turner, J.T., et al., 2007a. Springtime transport and retention of *Calanus finmarchicus* in Massachusetts and Cape Cod Bays, USA, and implications for right whale foraging. Mar. Ecol. Prog. Ser. 349, 183–197.

Jiang, M., Zhou, M., Libby, P.S., Hunt, C.D., 2007b. Influences of the Gulf of Maine intrusion on the Massachusetts Bay spring bloom: a comparison between 1998 and 2000. Cont. Shelf Res. 27, 2465–2485.

Jiang, M., Wallace, G.T., Zhou, M., et al., 2007c. Summer formation of a high nutrient and low oxygen pool in Cape Cod Bay. J. Geophys. Res. Oceans 112 (C5), C05006. http://dx.doi.org/10.1029/2006JC003889.

Jiang, M.S., Zhou, M., Anderson, D.A., Libby, P.S., 2011. Dynamics of a meso-scale eddy off Cape Ann, Massachusetts. Deep-Sea Res. I 58, 1130–1146.

Keller, A.A., Taylor, C., Oviatt, C., Dorrington, T., Holcombe, G., Reed, L., 2001. Phytoplankton production patterns in Massachusetts Bay and the absence of the 1998 winter–spring bloom. Mar. Biol. 138, 1051–1062.

Kilham, P., Hecky, R.E., 1988. Comparative ecology of freshwater and marine ecosystems. Limnol. Oceanogr. 33 (4), 776–795.

Lancelot, C., Rousseau, V., 1994. Ecology of *Phaeocystis*: the key role of colony forms. In: Green, J.C., Leadbeater, B.S.C. (Eds.), The Haptophyte Algae. Clarendon Press, Oxford, pp. 229–245.

Lancelot, C.G., Billen, A. Sournia, et al., 1987. *Phaeocystis* blooms and nutrient enrichment in the continental coastal zones of North Sea. Ambio 16 (1), 38–46.

Lancelot, C., et al., 2005. Modelling diatom and *Phaeocystis* blooms and nutrient cycles in the Southern Bight of the North Sea: the MIRO model. Mar. Ecol. Prog. Ser. 289, 63–78.

Lancelot, C., Gypens, N., Billen, G., Garnier, J., Roubeix, V., 2007. Testing an integrated river–ocean mathematical tool for linking marine eutrophication to land use: the *Phaeocystis*-dominated Belgian coastal zone (Southern North Sea) over the past 50 years. J. Mar. Syst. 64, 216–228.

Lancelot, C., Rousseau, V., Gypens, N., 2009. Ecologically based indicators for *Phaeocystis* disturbance in eutrophied Belgian coastal waters (Southern North Sea) based on field observations and ecological modeling. J. Sea Res. 61 (2009), 44–49.

Libby, P.S., Albro, C.S., Hunt, C.D., et al., 1999. 1998 Annual Water Column Monitoring Report. Massachusetts Water Resources Authority, Boston (Report 1999-16, 180 pp.).

Libby, P.S., Geyer, W.R., Keller, A.A., et al., 2007. Water Column Monitoring in Massachusetts Bay: 1992–2006. Massachusetts Water Resources Authority, Boston (Report 2007-11. 228).

Libby, P.S., Borkman, D.G., Geyer, W.R., et al., 2008. Water Column Monitoring in Massachusetts Bay: 1992–2007. Massachusetts Water Resources Authority, Boston (Report 2008-16. 170 pp.).

Lynch, D.R., Holboke, M.J., Naimie, C.E., 1997. The Maine coastal current: spring climatological circulation. Cont. Shelf Res. 17 (6), 605–634.

McArthur, R.H., Wilson, E.O., 1967. The Theory of Island Biogeography. Princeton University Press, Princeton, N. J.(203 pp.).

Nejstgaard, J., Tang, K., Steinke, M., Dutz, J., Koski, M., Antajan, E., Long, J., 2007. Zooplankton grazing on *Phaeocystis*: a quantitative review and future challenges. Biogeochemistry 83, 147–172.

Nelson, D.M., Smith, W.O., 1991. Sverdrup revisited: critical depths, maximum chlorophyll levels, and the control of Southern Ocean productivity by the irradiance-mixing regime. Limnol. Oceanogr. 36 (8), 1650–1661.

Officer, C.B., Ryther, J.H., 1980. The possible importance of silicon in marine eutrophication. Mar. Ecol. Prog. Ser. 3, 83–91.

Ohman, M.D., Runge, J.A., Durbin, E.G., Field, D.B., Niehoff, B., 2002. On the birth and death in the sea. Hydrobiologia 480, 55–68.

Ohman, M.D., Eiane, K., Durbin, E.G., et al., 2004. A comparative study of *Calanus finmarchicus* mortality patterns at five localities in the North Atlantic. ICES J. Mar. Sci. 61 (4), 687–697.

Ohman, M.D., Durbin, E.G., Runge, J.A., et al., 2008. Relationship of predation potential to mortality of *Calanus finmarchicus* on Georges Bank, northwest Atlantic. Limnol. Oceanogr. 53 (4), 1643–1655.

Oviatt, C.A., Hyde, K.J.W., Keller, A.A., et al., 2007. Production patterns in Massachusetts Bay with outfall relocation. Estuar. Coasts 30 (1), 35–46.

Peperzak, J., Coljn, L.F., Gieskes, W.W.C., et al., 1998. Development of the diatom-*Phaeocystis* spring bloom in the Dutch coastal zone of the North Sea: the silicon depletion versus the daily irradiance threshold hypothesis. J. Plankton Res. 20 (3), 517–537.

Petrie, B., Drinkwater, K., 1993. Temperature and salinity variability on the Scotian Shelf and in the Gulf of Maine 1945–1990. J. Geophys. Res. 98 (C11), 20,079–20,089.

Pettigrew, N.R., Churchill, J.H., Janzen, C.D., et al., 2005. The kinematic and hydrographic structure of the Gulf of Maine Coastal Current. Deep-Sea Res. II 52, 2369–2391.

Platt, T., Gallegos, C.L., Harrison, W.G., 1980. Photoinhibition of photosynthesis in natural assemblages of marine phytoplankton. J. Mar. Res. 38 (4), 687–701.

Ramp, S., Schlitz, R., Wright, W., 1985. The deep flow through the Northeast Channel, Gulf of Maine. J. Phys. Oceanogr. 15, 1790–1808.

Rogers, S.I., Lockwood, S.J., 1990. Observations of coastal fish fauna during a spring bloom of *Phaeocystis pouchetii* in the Eastern Irish Sea. J. Mar. Biol. Assoc. U. K. 70, 249–253.

Sarthou, G., et al., 2005. Growth physiology and fate of diatoms in the ocean: a review. J. Sea Res. 53, 25–42.

Schoemann, V., Becquevort, S., Stefels, J., Rousseau, V., Lancelot, C., 2005. *Phaeocystis* blooms in the global ocean and their controlling mechanisms: a review. J. Sea Res. 53, 43–66.

Smith Jr., W.O., Codispoti, L.A., Nelson, D.M., et al., 1991. Importance of *Phaeocystis* blooms in the high-latitude ocean carbon cycle. Nature 352, 514–516.
Spilmont, N., et al., 2009. Impact of the *Phaeocystis globosa* spring bloom on the intertidal benthic compartment in the eastern English Channel: a synthesis. Mar. Pollut. Bull. 58, 55–63.
Stabell, O.B., Aanesen, R.T., Eilertsen, H.C., 1999. Toxic peculiarities of the marine alga *Phaeocystis pouchetii* detected by in vivo and in vitro bioassay methods. Aquat. Toxicol. 44, 279–288.
Steele, J.H., Henderson, E.W., 1992. The role of predation in plankton models. J. Plankton Res. 14 (1), 157–172.
Stefels, J., 1997. The Smell of the Sea: Production of Dimethylsulphoniopropionate and its Conversion into Dimethylsulphide by the Marine Phytoplankton Genus *Phaeocystis*. Ph.D. Thesis University of Groningen (147 pp.).
Tilman, D., 1977. Resource competition between planktonic algae: an experimental and theoretical approach. Ecology 58, 338–348.
Tilman, D., 1982. Resource Competition and Community Structure. Princeton University Press, Princeton, NJ (296 pp.).
Tootle, G.A., Piechota, T.C., Singh, A., 2005. Coupled oceanic–atmospheric variability and U.S. stream flow. Water Resour. Res. 41, W12408. http://dx.doi.org/10.1029/2005WR004381.
Townsend, D.W., Ellis, W.G., 2010. Primary production and nutrient cycling on the Northwest Atlantic continental shelf. In: Liu, K.K., Atkinson, L., Quinones, R., Talaue McManus, L. (Eds.), Carbon and Nutrient Fluxes in Continental Margins: A Global Synthesis. Springer Verlag, New York.
Townsend, D.W., Keller, M.D., 1996. Dimethylsulfide (DMS) and dimethylsulfoniopropionate (DMSP) in relation to phytoplankton in the Gulf of Maine. Mar. Ecol. Prog. Ser. 137 (1–3), 229–241.
Townsend, D.W., Keller, M.D., Sieracki, M.E., Ackleson, S.G., 1992. Spring phytoplankton blooms in the absence of vertical water columns stratification. Nature 360, 59–62.
Townsend, D.W., Cammen, L.M., Holligan, P.M., Campbell, D.E., Pettigrew, N.R., 1994. Causes and consequences of variability in the timing of spring phytoplankton blooms. Deep-Sea Res. I 41 (5–6), 746–765.
Townsend, D.W., Pettigrew, N.R., Thomas, A.C., 2005. On the nature of Alexandrium fundyense blooms in the Gulf of Maine. Deep-Sea Research II, 52. http://dx.doi.org/10.1016/j.dsr2.2005.06.028.
Townsend, D.W., et al., 2010. A changing nutrient regime in the Gulf of Maine. Cont. Shelf Res. 30, 820–832.
Turner, R.E., Qureshi, N., Rabalais, N.N., Dortch, Q., Justic, D., Shaw, R.F., Cope, J., 1998. Fluctuating silicate:nitrate ratios and coastal plankton food webs. Proc. Natl. Acad. Sci. U. S. A. 95, 13,048–13,051.
Turner, J.T., Borkman, D.G., Hunt, C.D., 2006. Zooplankton of Massachusetts Bay, USA, 1992–2003: relationships between the copepod *Calanus finmarchicus* and the North Atlantic Oscillation. Mar. Ecol. Prog. Ser. 311, 115–224.
Turpin, D.H., Harrison, P.J., 1979. Limiting nutrient patchiness and its role in phytoplankton ecology. J. Exp. Mar. Ecol. 39, 151–166.
Utermöhl, H., 1958. Zur Vervollkommnung der quantitativen phytoplankton-methodikk. Mitt. Int. Ver. Theor. Angew. Limnol. 9, 1–38.
van Rijssel, A., Alderkamp, M.A., Nejstgaard, J.C., Sazhin, A.F., Verity, P.G., 2007. Haemolytic activity of live *Phaeocystis pouchetii* during mesocosm blooms. Biogeochemistry 83, 189–200. http://dx.doi.org/10.1007/s10533-007-9095-1.
Veldhuis, M.J.M., Colijn, F., Admiraal, W., 1991. Phosphate utilization in *Phaeocystis pouchetii* (*Haptophyceae*). Mar. Ecol. 12 (1), 53–62.
Walsh, J.J., Dieterle, D.A., Lenes, J., 2001. A numerical analysis of carbon dynamics of the Southern Ocean phytoplankton community: the roles of light and grazing in effecting both sequestration of atmospheric CO_2 and food availability to larval krill. Deep-Sea Res. 48, 1–48.
Walsh, J.J., Dieterle, D.A., Maslowski, W., Whitledge, T.E., 2004. Decadal shifts in biophysical forcing of Arctic marine food webs: numerical consequences. J. Geophys. Res. Oceans 109, C05031. http://dx.doi.org/10.1029/2003JC001945.
Wheeler, P.A., Kokkinakis, S.A., 1990. Ammonium recycling limits nitrate use in the oceanic subarctic Pacific. Limnol. Oceanogr. 35 (6), 1267–1278.
Whipple, S.J., et al., 2007. Gaining integrated understanding of *Phaeocystis* spp. (*Prymnesiophyceae*) through model-driven laboratory and mesocosm studies. Biogeochemistry 83, 293–309.
Wilson, J.B., Spijkerman, E., Huisman, J., 2007. Is there really insufficient support for Tilman's R^* concept? A comment on Miller et al. Am. Nat. 169 (5), 700–706.
Wu, D., 2011. NPDES Compliance Summary Report, Fiscal Year 2010. Massachusetts Water Resources Authority, Boston (Report 2011-06. 145 pp.).